



NextGEM

Next Generation Integrated Sensing and Analytical System for Monitoring and Assessing Radiofrequency Electromagnetic Field Exposure and Health

D4.5: Biochemical and biophysical mechanisms in EMF - Final report

Document Summary Information

Start Date	01/07/2022	Duration	48 months
Project URL	https://www.nextgem.eu/		
Deliverable	D4.5: Biochemical and biophysical mechanisms in EMF - Final report		
Work Package	WP4	Task	T4.1
Contractual due date	30/09/2024	Actual submission date	30/09/2024
Type	Report	Dissemination Level	PU - Public
Lead Beneficiary	UZH	Deliverable Editor	Anna Bogdanova (UZH)



This project has received funding from the European Union's Horizon Europe research and innovation programme under the Grant Agreement No 101057527

Contributors and Peer Reviewers

Contributors
Anna Bogdanova (UZH), Yuri Feldman, Igal Bilik, Gregory Barshterin (HUJI), Olga Zeni (CNR), Maryse Ledent (SC), Fulvio Schettino (UCAS), Marco Spirito (TUD), Nikolaos Petroulakis (FORTH)
Peer Reviewers
Maryse Ledent (SC), Olga Zeni (CNR)

Revision history (including peer-reviewing and quality control)

Version	Issue Date	Changes	Contributor(s)
v0.1	23/06/2024	Table of Contents provided	Anna Bogdanova (UZH)
v0.2	15/07/2024	Sections populated with the Task leaders	Anna Bogdanova (UZH), Olga Zeni (CNR)
v0.3	22/07/2024	Section defined, assigned, and agreed	Anna Bogdanova (UZH), Olga Zeni (CNR)
v0.4	05/08/2024	First contributions	All partners
v0.5	25/08/2024	Integration and harmonization	Anna Bogdanova (UZH)
v0.6	10/9/2024	Second contributions and updates	All partners
v0.7	13/09/2024	Complete version ready for peer review	Anna Bogdanova (UZH), Nikolaos Petroulakis (FORTH)
v0.8	22/09/2024	Peer review	Maryse Ledent (SC), Olga Zeni (CNR)
v0.9	27/09/2024	Comments addressed from peer review, technical and quality assurance	Mats-Olof Mattsson (SPi), Kyriaki Psara (eBOS), Anna Bogdanova (UZH), Panos Chatziadam (FORTH)
v1.0	30/09/2024	Final review and submission	Nikolaos Petroulakis (FORTH)

Disclaimer

Funded by the European Union. Views and opinions expressed are however those of the author(s) only and do not necessarily reflect those of the European Union or the European Commission. Neither the European Union nor the granting authority can be held responsible for them.”

While the information contained in the documents is believed to be accurate, the authors(s) or any other participant in the NextGEM consortium make no warranty of any kind with regard to this material including, but not limited to the implied warranties of merchantability and fitness for a particular purpose.

Neither the NextGEM Consortium nor any of its members, their officers, employees, or agents shall be responsible or liable in negligence or otherwise howsoever in respect of any inaccuracy or omission herein.

Without derogating from the generality of the foregoing neither the NextGEM Consortium nor any of its members, their officers, employees, or agents shall be liable for any direct or indirect or consequential loss or damage caused by or arising from any information advice or inaccuracy or omission herein.

Copyright message

© NextGEM Consortium. This deliverable contains original unpublished work except where clearly indicated otherwise. Acknowledgement of previously published material and of the work of others has been made through appropriate citation, quotation, or both. Reproduction is authorised provided the source is acknowledged.

Table of Contents

Executive Summary.....	9
1 Introduction.....	10
1.1 Mapping NextGEM Outputs	10
1.2 Deliverable overview and report structure	10
1.3 Update from previous Deliverable D4.1 “Biochemical and biophysical mechanisms in EMF - Initial report”.....	11
2 Background.....	12
2.1 Biophysical and biochemical mechanisms of interaction between RF-EMF and biological systems.....	12
2.1.1 State of art understanding of the physics of interaction of the RF-EMF with living cells.....	12
2.1.2 Thermal effects of RF-EMF for biomolecules to cells and organisms. Temperature-dependent processes in biological systems.....	12
2.1.3 Non-thermal effects of the RF-EMF	13
2.2 Mechanisms of interaction of RF-EMF at the cellular level	14
2.2.1 General considerations on the presumably non-thermal responses of cells to RF-RMF.....	14
2.2.2 Red blood cells and their components as a model to study mechanisms of interaction between RF-EMF and biological systems.....	16
3 New EMF exposure setups for red blood cells in flow	18
3.1 Exposure setup for the far-field mode of exposure to the RF-EMF of 3.5 GHz.....	18
3.1.1 Equipment and Materials.....	18
3.2 Unified signal to expose biological samples and the generator/interface to produce it	21
4 Temperature-dependence of the parameters of interest	24
4.1 Kinetics of thiol-disulfide exchange reaction between the oxidised glutathione (GSSG) and reduced thiols of hemoglobin molecule.....	24
4.1.1 Introduction	24
4.1.2 Experimental procedures	25
4.1.3 Results and discussion.....	25
4.2 Effect of temperature on the intraerythrocytic Ca^{2+} levels.....	26
4.2.1 Introduction	26
4.2.2 Methodology	26
4.2.3 Results and discussion.....	27
4.3 Temperature effects on RBC deformability.....	28
4.3.1 Introduction	28
4.3.2 Methodology.....	28
4.3.3 Results and discussion.....	28
4.4 Temperature effects on nitric monoxide production by RBCs.....	31
4.4.1 Introduction	31
4.4.2 Methods.....	31
5 Conclusion	32

References 33

List of Figures

Figure 1: Far-Field EMF Exposure Cell (3D printed), dimensions shown are in mm.	18
Figure 2: Scheme of the protective cover with diminutions set for the 3.5 GHz frequency.	19
Figure 3: Physical (A) and schematic representation of the antenna (A) top and bottom views; (B) antenna's geometry.	19
Figure 4: CST simulation for the exposure cuvette (A), CST Simulation of the plane-wave ~3.5 GHz, distance between the antenna and the sample's brim is 4λ (B) and simulation of the plane-wave 26 GHz, distance between the antenna and the sample's brim is fixed at 4λ (C).	20
Figure 5: SAR distribution in the blood sample based on the CST simulation for the 3.5 GHz (A) and the 26 GHz (B). (A): On the left – the simulation setup. The cuvette filled with blood at 37 °C with patch antenna located at 4λ distance above the blood sample brim. The middle and right panels represent the SAR distribution in the sample, top-side view and a cut-side view, respectively. (B): SAR distribution at 26 GHz with a plane wave source, located at a distance of 4λ. We used the Microwave Dielectric Spectroscopy method to control the EMF exposure effect.	21
Figure 6: Signals temporarily used and the unified signal to be used in the future in the biological experiments. (A) The signal used for RBC sample is a squared pulse, modulated with the sinus of the 900MHz, 1GHz and 3.5GHz. The pulse width of 100 microsec and the duty cycle of 10% was used. The signal power was 10dBm at the output of the signal generator port. (B) RF modulation (simplified) concept, described in the (Ba) time domain and (Bb) frequency domain. (C) I and Q waveform of data modulated using a QAM (Ca) and an OFDM modulation (Cb). (D) I and Q time domain waveform of 5G NR test model 3.1.....	22
Figure 7: A sequence of thiol oxidation steps where sulfur (S) changes its oxidation state from -2 to +4.	24
Figure 8: Temperature-dependence of S-glutathionylation of hemoglobin. The abundance of S-glutathionylated adducts is shown after 3 or 15 min of incubation of hemolysate with GSSG at 2, 25 or 37°C. Presented are the examples of immunoblots and the outcome of densitometry normalized to the Hb loading control. "Lysate" stands for the basal S-glutathionylation of Hb before the addition of GSSG. * denotes p<0.05 in One-way Anova on repeated measures. Data are results of 3 independent experiments ±SD.	26
Figure 9: Temperature-dependence of intracellular free Ca ²⁺ in RBCs. RBCs were incubated at designated temperature for 20 or 40 min and intracellular Ca ²⁺ was then assessed by means of flow cytometry using Fluo-4 AM as a Ca ²⁺ -dependent fluorescent marker. * denotes p<0.05 in One-way Anova on repeated measures. Data are results of 3 independent experiments ±SD. Shown in panel B are the negative and the positive controls. Panel C gives an example of a functional test in which the maximal activity of Piezo1 channels and the functionality of the PMCA are shown. Yoda is the activator of Piezo1 channel. BAPTA is a chelator of intracellular Ca ²⁺ and serves as a negative control. Amplitude of Ca ²⁺ accumulation and the kinetics of Ca ²⁺ extrusion are associated with the increase or decrease in fluorescence intensity of Ca ²⁺ -sensitive fluorescent dye fluo-4.....	27
Figure 10: Temperature-dependence of forward and side scatter measured by flowcytometry. * denotes p<0.05 in One-way Anova on repeated measures. Data are results of 3 independent experiments ±SD.	29
Figure 11: Temperature-dependence of the osmoscan parameters obtained using Lorrca red blood cell analyzer. Shown in the figure are half-maximal and minimal tolerated osmolarities O _{hyper} (A) and O _{min} (B) as well as optimal osmolarity (O _{EImax} , C) and maximal elongation index (EI _{max} , D). Readouts obtained at the shear stress of 30 Pa. Results are means ±SD of three independent experiments.....	29
Figure 12: Temperature-dependence of RBC deformability presented as elongation index at different intensity of shear stress. Data are results of 3 independent experiments ±SD.	30

List of Tables

Table 1: Adherence to NextGEM’s GA Tasks and Deliverables Descriptions 10

Table 2: Unified signal characteristics.....23

Table 3: Alteration of RBC deformability parameters after incubation of RBCs under 40°C (data are results of 3 independent experiments \pm SD)30

Glossary of terms and abbreviations used

Abbreviation / Term	Description
ATP	Adenosine TriPhosphate
ATPase	Adenosine TriPhosphatase
CCCP	Carbonyl cyanide m-chloro-phenylhydrazone
DIBAC4(5)	Bis(1,3-dibutylbarbituric acid)
EMF	Electromagnetic Field
ES	Effects Size
ESR	Erythrocyte Sedimentation Rate
GSH	Reduced glutathione
GSM	Global System for Mobile Communications
GSSG	Oxidized glutathione
HaCaT	Human epidermal keratinocyte line
Hb	Hemoglobin
HSF	Heat Shock Factor
HSP	Heat Shock Protein
HUJI	The Hebrew University of Jerusalem
HW	Hardware
ICNIRP	International Commission on Non-Ionizing Radiation Protection
LUT	Liquid Under Treatment
Met-Hb	Met-hemoglobin
NADPH	Nicotinamide Adenine Dinucleotide Phosphate
NextGEM	Next Generation Integrated Sensing and Analytical System for Monitoring and Assessing Radiofrequency Electromagnetic Field Exposure and Health
NMDA	N-methyl D-aspartate
NO	Nitric Oxide
NOS	Nitric Oxide Synthase
OFDM	Orthogonal Frequency Division Multiplexing

PIEZO1	Mechanosensitive nonselective cation channel
PMCA	Plasma membrane Ca^{2+} ATPase
QAM	Quadrature Amplitude Modulation
RBC	Red Blood Cells
RF-EMF	RadioFrequency ElectroMagnetic Field
SAR	Specific Absorption Rate
SCHEER	Scientific Committee on Health, Environmental and Emerging Risks
SH-SY5Y	Human neuroblastoma cell line
SOPs	Standard Operation Procedures
TEM	Transverse Electromagnetic
TRP(C)	Transient Receptor Potential (channel)
TRPV	Transient Receptor Potential Vanilloid
THUAS	The Hague University of Applied Sciences
TUD	Technische Universiteit Delft
UCAS	University of Cassino e del Lazio Meridionale
VGCC	Voltage-Gated Cation Channel
V _{max}	Maximum turnover rate
WHO	World Health Organization
WP	Work package

Executive Summary

Deliverable D4.5 provides an overview of the current state of research focusing on the characterization of biochemical and biophysical mechanisms of electromagnetic fields (EMF) interaction with biological systems, as obtained by the NextGEM consortium.

Investigating the basic physical and chemical processes initiated in living systems upon exposure to EMF in the radiofrequency (RF) range (RF-EMF) is one of the goals of the NextGEM project. These processes, reviewed in more detail in D4.1, include thermal and possibly non-thermal responses of water, proteins, and lipids to the microwave-modulated EMF signal [1][2][3]. We selected red blood cells (RBCs) as a model cell system to explore the effects of EMF. A challenge in monitoring the RBC response to EMF exposure is the need to use perfusion circuits to mimic blood flow through vessels *ex vivo*, whereas the currently used exposure setups are static and primarily assess the behaviour of cell lines in Petri dishes under exposure conditions. Thus, the main work within Task 4.1 over the past months focused on improving the prototype of the exposure system. We also examined the possible thermal components of the responses of model systems and processes to EMF.

This deliverable is based on work performed within Task 4.1. However, it also includes the development of the definitive design of the pilot study, in which the blood of healthy volunteers exposed locally to a signal simulating that emitted by mobile phones will be tested for responsiveness to RF-EMF in a setting typical of 5G NR.

In this deliverable, we introduce a new exposure setup and some pilot data obtained using the first prototype. Further improvements to the prototype include the reduction of RBC damage by the peristaltic pump, and automation of volume and temperature control in the exposure chamber. These findings are discussed in the context of the current understanding of the biochemical and biophysical mechanisms between RF-EMF and biological systems. This overview of complex biological responses and the possible mechanisms of interaction at the cellular level provides the background for the experimental activities of Task 4.1 and links to the other tasks within WP4 and case studies.

1 Introduction

Radiofrequency electromagnetic fields (RF-EMF) in the 100MHz-300GHz frequency range are now employed worldwide in a variety of technologies. The exposure of humans as well as other species and the environment worldwide to the EMF is unavoidable. Fast development of the new technologies and their deployment, including 5G and the upcoming 6G communication networks has long overrun the pace of studies on the potential health risks to humans and other species. The increasing public concern for possible health risks gave rise to EU initiatives focusing on the systematic investigation of the processes underlying the interaction of the RF-EMF with biological systems, analysis of the existing information and, when needed, re-evaluation of the existing safety guidelines. Until now, several biological effects of RF-EMF exposure involving thermal and, possibly, non-thermal mechanisms are described and discussed by the scientific community. Tissue heating is the only established effect of exposure to RF-EMF, for which exposure limits have been defined [4]. On the contrary, non-thermal mechanisms have not been clarified yet. A few hypotheses have been suggested, but none of them has been “proven” so far. Thus, it remains unclear if the non-thermal effects of RF-EMF exist. The studies to substantiate their role in the reported biological and health effects of the field are on-going across different research domains, from experimental studies to epidemiological research [5][6][7][8][9][10][11].

1.1 Mapping NextGEM Outputs

The purpose of this section is to map NextGEM’s Grant Agreement (GA) commitments, both within the formal Task description and Deliverable, against the project’s respective outputs and work performed.

Table 1: Adherence to NextGEM’s GA Tasks and Deliverables Descriptions

TASKS	
Task Number & Title	Respective extract from formal Task Description
Task 4.1 - Biochemical and Biophysical mechanisms of EMF responses	Numerous reports on the non-thermal effects of EMF on living cells usually refer to the description of the changes in protein expression and cellular functions, whereas the chemical and biophysical mechanisms of these processes remain less explored. Therefore, we shall study the impact of EMF (carrier frequencies and the envelope) on the state of water in protein solutions (dielectric spectroscopy), by means of special sample holder combined with a transverse electromagnetic field (TEM), with the subsequent assessment of dielectric parameters. Readouts on the changes in free to bound water will be followed by the analysis of the chemical and biophysical processes on Haemoglobin (Hb). The impact of EMF on kinetics of Hb modifications will be monitored to assess possible proton dissociations, and on the surface charge of Hb. Possible effects on Hb, RBC-membrane, intact RBC-suspension, and in whole blood will provide information of exposure conditions that causes responses to be applied to other cell types used by other partners.
DELIVERABLE	
Deliverable: D4.5: Biochemical and biophysical mechanisms in EMF – Final report (M27) This deliverable will provide the final report of possible effects (A) on intracellular water state, protein modifications and membrane properties (B) on proteins and plasma membranes in intact cells.	

1.2 Deliverable overview and report structure

Based on the objectives and work carried out under Task 4.1, the document starts with the Executive Summary followed by the introduction of the document in Section 1.

Section 2 “Background” is an extended version of the information on the physical, chemical and biological processes initiated in the living systems by RF-EMF exposures.

Section 3 is dedicated to the progress in design, construction and characterisation of the exposure setup mimicking far-field conditions of exposure of blood cells and cell components to microwave EMF in flow. Unified signal properties are also covered in this section.

Section 4 follows up on the responses of selected RBC parameters to changes due to temperature. Those include kinetics of thiol-disulfide exchange between hemoglobin thiols and oxidized glutathione, Ca^{2+} dynamics in red blood cells and their rheological properties.

Section 5 provides conclusions and the outlook for the future activities within Work Package 4.

1.3 Update from previous Deliverable D4.1 “Biochemical and biophysical mechanisms in EMF - Initial report”

This deliverable provides a follow-up on the deliverable D4.1. It reflects the deviations from the initial plan to explore the effect of the RF-EMF on the RBC properties such as the state of water in the cells, RBC deformability and aggregability as well as on the Ca^{2+} uptake by the ion channels (section 4 of deliverable D4.1) and NO production by the erythroid NO synthase and on the redox state and reversible thiol modifications of hemoglobin (Section 5 of deliverable D4.1) during the period from M17 to M23 of the NextGEM project life-span. We have investigated the thermal responses of some of these parameters in order to be able to compare the observed thermal responses with those induced by exposure to the microwave EMF. At present we have explored temperature-dependence of:

- The kinetics of S-glutathionylation reaction, described in Section 4.2.1 of deliverable D4.1 and updated in Section 4.1 of the present deliverable D4.5;
- Ca^{2+} movements through the RBC membranes, Section 4.1.3 of deliverable D4.1 updated in Section 4.2 of the present deliverable D4.5;
- Deformability referred to in Section 5.2 of deliverable D4.1 and updated in the Section 4.3 of the present deliverable D4.5.
- We are providing information on the temperature-dependence of NO production (Section 4.2.3 of deliverable D4.1 and Section 4.4 of the present deliverable D4.5).

2 Background

2.1 Biophysical and biochemical mechanisms of interaction between RF-EMF and biological systems

2.1.1 State of art understanding of the physics of interaction of the RF-EMF with living cells

When a RF-EMF impinges on a living cell or a multicellular organism, it is partly reflected, partly transmitted, refracted, or scattered. The transmitted and refracted fields from the RF-EMF exposure induce electric and magnetic fields within the biological systems that interact with cells and tissues in a variety of ways, resulting in complex patterns of EMF distribution inside the system that are heavily dependent on the EMF characteristics (frequency, waveform, and strength of the induced fields), as well as the physical properties and dimensions of the body [4][12].

Thus, the EMF does not only interact with the biological systems but also causes changes within the cells that can be observed as rather complex biological responses [13]. The understanding of biophysical and biochemical mechanisms of interaction between RF-EMF and biological systems is of pivotal importance for health risk assessment, and prediction of possible ecological consequences of deployment 5G and subsequent communication technologies.

RF-EMF radiation is transmitted by low-energy photons that do not produce ionization of the biological molecules and belong to the “non-ionizing radiation” type. Instead, RF-EMF induces relaxation phenomena in the biological systems by acting on the polar molecules, including water as well as charged or polarized micro- and macromolecules, macromolecular complexes that build the cells. Charged membrane surfaces also interact with non-ionizing RF-EMF. The sinusoidal electric field causes rotation and tumbling of polar molecules. These movements do not occur instantaneously due to the inertia and viscous forces exerted by the media in which they are immersed, giving rise to a time-dependent behavior known as the relaxation process [14][15][16][17][18]. Moreover, cells and subcellular structures (organelles, plasma membrane), as well as organic and inorganic ions in the cytosol carry different electric charges. When subjected to electrical stimulation, they require a finite amount of time for the charges to accumulate at the interfaces and to equilibrate. The accumulation of charges at the interfaces continues until a condition of equilibrium is re-established, leading to the relaxation phenomenon [19].

Interactions between RF-EMF and biological systems resulting in “biological effects” are attributed to thermal or, possibly, also non-thermal causes.

2.1.2 Thermal effects of RF-EMF for biomolecules to cells and organisms. Temperature-dependent processes in biological systems

Thermal effects are mainly associated with the absorption of the RF energy resulting from the electrical conductivity and dielectric losses of most biological media. The pulsed electric field generates an oscillating current, and the energy is rapidly transferred into the motion of water molecules, which ultimately induces an increase in local temperature (dielectric heating) as in the microwave oven [19].

To understand the possible impact of heating of the cells and tissues in response to RF-EMF exposure, it is important to evaluate the effects of temperature per se on biochemical and physiological processes. Most of the reactions in biological systems are associated with the consumption or release of heat (exothermic or endothermic in nature) and, hence, kinetics of these reactions are influenced by the changes in temperature. In the cells, these responses are orchestrated in a way that allow different species to survive and adapt to the changes in ambient and body temperature [20]. Marked species-specific differences are therefore reported for the hibernating and non-hibernating mammals to say nothing about the variations between the animals with constant body temperature and those that cannot maintain it (homeothermic vs poikilothermic species). In human RBCs, increase in temperature results in higher glucose uptake and an increase in maximal transport rate (V_{max}) along with a decrease in affinity (increase in K_m) for glucose transporter [21][22]. Facilitated ATP production covers the rising energy expenditure as increase in temperature results in activation of ion transport ATPases [23]. Activation of the pumps is required to maintain transmembrane ion gradients since passive Na^+ and K^+ transport across the membrane of human RBCs also increases [23][24][25]. Na,K -ATPase was shown to be activated with an increase in temperature within sublethal range [23]. However, exposure of RBCs to 2.45 GHz microwave radiation at a dose of 6 W/kg was reported to suppress the Na,K -ATPase activity by 35% which was claimed to be due to a thermal effect of the EMF [26]. Little is known about the temperature-dependence of passive Ca^{2+} transport in human RBCs. However, extrusion of Ca^{2+} from red blood cells mediated by plasma membrane Ca^{2+} ATPase is

known to be facilitated with increasing temperature [27]. Reports on the impact of microwave radiation on passive Ca^{2+} uptake and its extrusion mediated by the Ca^{2+} pumps are rather contradictory, and dependent on the type of tissue, type of signal and on the methods of detection of Ca^{2+} movements through the membrane [28]. Taken together, thermal effects on RBCs may influence ion transport across the membrane and cause changes in RBC volume, deformability and in the intracellular Ca^{2+} -dependent signalling. Interaction between the thermal and possibly non-thermal components remain to be investigated.

Physical and physico-chemical processes make O_2 availability temperature-dependent. Oxygen affinity of hemoglobin is temperature-sensitive as O_2 binding to hemoglobin is an exothermic reaction [29]. Solubility of O_2 in water is decreasing with increase in temperature. As a result, heating may promote hypoxia. Induction of hypoxia by RF-EMF was reported in tumors in rodent models in which electrochemotherapy was simulated [30][31]. Deoxygenation in turn results in the electron leak from the mitochondrial electron transduction chain and free radical burst [32]. Furthermore, rising temperature facilitates NO production [33][34][35][36][37][38][39][40]. Aggregation [41] and deformability of RBCs [42] are temperature-sensitive.

Heating regulates gene expression response which is orchestrated by heat-shock transcription factors [43]. The heat-shock factor (HSF) activation cycle is initiated by dissociation of the HSF monomers from their complexes with the inhibitory heat-shock proteins (HSP) 40, 70 or 90, its translocation to the nucleus and trimerization. When in the nucleus, the trimers recruit co-activators and interact with the heat-shock response elements at the DNA and initiate the production of chaperones, co-chaperones and polyubiquitin. Expression of these proteins is required to tackle protein unfolding and denaturation in response to heating. The targets of HSF include the HSP 40, 70 and 90 that interact with HSF and inactivate them providing a feedback loop and suppressing heat shock gene expression response [43].

Taken together, responses of the living organisms to sublethal heating are complex and multifactorial, and may include alterations in ion transport, increase in energy expenditure, deoxygenation, as well as to oxidative stress secondary to hypoxia. When persisting these biological responses may result in the development of pathologies including cancer progression or neurodegenerative diseases [44].

In fact, multiple reports on the RF-EMF interaction with biological systems may be associated with heat-stress response or oxidative damage which are referred to as possible non-thermal responses [45][46][47]. Heating may contribute to these responses as well. However, induction of heat-shock response as well as of other types of responses strongly depends on the experimental settings (types of cells, duration of exposure, power and frequency as well as the presence of modulation of RF-EMF signal) [48]. Furthermore, modulation of responsiveness to hypoxia along with and induction or suppression of HSP70 expression could be observed in chick embryos exposed to a modulated 0.915 GHz signal [48].

International guidelines limiting human exposure to RF-EMF are based largely on the well-known thermal effects of these fields [4].

2.1.3 Non-thermal effects of the RF-EMF

Molecular mechanisms of non-thermal effects remain a matter of debates. They are not directly associated with this temperature change but rather with some other processes induced by the RF electric or magnetic field at different levels of the biological scale of complexity. A literature overview covering this research area is presented in D4.1. It includes an overview of potential mechanisms of action of EMF on atoms, molecules and cells provided by Apollonio et al. [13].

At the subatomic level, the magnetic field (MF) interferes with biochemical reactions involving radical pairs. Free radicals are molecules with an unpaired electron, normally highly reactive and short-lived. They are usually generated in pairs as intermediates in chemical reactions, and free radicals are produced if the radical pair dissociates before the two radicals can recombine. The electron pairs formed as intermediates can be produced either with their spins antiparallel or parallel and oscillate between these two configurations at a rate determined by the hyperfine coupling. They are less likely to recombine and hence more likely to dissociate into free radicals if they are in the parallel spin state. It is hypothesized that the interaction with an exogenous MF can change the probability of radical pairs recombination, thus altering the reaction equilibrium [49]. Even though this mechanism is usually associated with the action of static or low-frequency magnetic fields, also pulsed RF-EMF has been reported to shift the equilibrium and, hence, potential, which has an important role in several diseases, including cancer [50].

At the level of macromolecules, one of the most studied hypotheses of interaction with RF fields is the possibility of inducing conformational changes in proteins, such as enzymes, ionic channels, and pumps [46][51]. The significance of this mechanism lies in the fact that the efficiency of the protein in eliciting a specific function strictly

depends on its conformation. Therefore, such conformational changes could lead to alterations in important biochemical processes [13][19].

It has been hypothesized that changes in protein conformation could be related to:

1. The direct action of the electric field (EF) on the protein dipole moments [6][13].
2. The resonant energy absorption by intrinsic protein modes. Depending on the protein conformation, a number of both vibrational and torsional modes can be excited. It is suggested that such dynamic modes can be excited by low-level RF-EMF [6][13][19].
3. Transient heating of the protein and its environment [52].
4. Changes in mobility and abundance of water molecules in the hydration shell of a protein. Changes in proton/hydronium mobility and local pH changes [17][53].
5. Interference of RF-EMF into the process of enzymatic (e.g., by NADPH oxidases, NO synthases or mitochondrial electron transduction chain complexes) and non-enzymatic (hydroxyl radical production in Fenton reaction or interaction of superoxide anion with NO)) free radical production due to the free radical pair electron spin-polarization [46][47][50].

2.2 Mechanisms of interaction of RF-EMF at the cellular level

2.2.1 General considerations on the presumably non-thermal responses of cells to RF-RMF

The main interest in studying how EMF interact with cells and their environment, is to identify the real effects of these fields in cellular function and the direct and indirect risks to human health. To date, the most investigated critical conditions that could provide evidence of a mechanism at the cellular level by which RF exposure might affect human health are oxidative stress, genotoxicity, effects on calcium signalling and voltage-gated channels, and on apoptosis.

Oxidative stress occurs when the production of oxidants overrides the antioxidant capability of the cells. As a result, the oxidants react with macromolecules like proteins, lipids and nucleic acids giving rise to an alteration in cellular functions related to several diseases like cancer and neurodegenerative diseases [54]. Genotoxicity is one of the key biological indicators of carcinogenicity and the most common characteristic of established carcinogens [55]. The role for Ca^{2+} as a signalling molecule underlying the non-thermal interaction of RF EMF has been hypothesized due to the involvement of calcium signalling pathways in the regulation of many essential cellular processes [56][57][58]. Apoptosis is an important cell death program, highly conserved within multicellular organisms and genetically controlled, which is responsible for the removal of damaged, dysfunctional, or no longer necessary cells to promote homeostasis and the survival of organisms [59].

Results of the studies on the possible cancerogenic action of RF-EMF are conflicting: some studies found evidence that could demonstrate the involvement of these cellular functions, while others did not. Such conflicting results makes it difficult to draw meaningful conclusions. A valid approach is to consider systematic reviews and meta-analysis, and in case these are not available, good quality review papers can be also considered. A good quality review paper applies a systematic literature search and includes single studies adhering to basic quality criteria defined a priori. In such a way, the risk of bias is reduced. The conclusions of the review are reliable and do not represent the personal opinion of the authors. This is the approach followed by the working group on electromagnetic fields of the Scientific Committee on Health Environmental and Emerging Health Risk (SCHEER) which, on request by the European Commission services, provides Opinions on questions concerning health, environmental and emerging risks. Regarding the evidence on interaction mechanisms at cellular level by which RF exposure might affect human health, the conclusion of the SCHEER is that there is uncertain weight of evidence for interaction mechanisms involving oxidative balance, genetic and epigenetic effects and calcium signalling that can result in biological effects [4]. A summary of the review papers analysed in the SCHEER Opinion, and the ones published after this Opinion, is provided below.

The narrative review by Schuermann and Mevissen [47] reports on key experimental findings on oxidative stress deriving from *in vivo* and *in vitro* studies published in the last decade. The results are discussed in the context of molecular mechanisms that can be relevant for human health, specifically for the impact on the nervous system, on the reproduction, and on blood and the immune system. They concluded on the increased oxidative stress due to RF EMF as from the majority of animal studies and from half of the cellular studies, but they pointed out that some studies were subjected to methodological uncertainties or were not very comprehensive regarding exposure time, SAR level, number and quantitative analysis of the endpoints analysed. Authors stated that standardized conditions are mandatory to better understand and confirm their conclusions. A systematic review, commissioned by World Health Organization (WHO), is recently published evaluating the associations between the exposure to

RF-EMF and oxidative stress in experimental models both *in vivo* and *in vitro* [60]. The protocol, presenting the detailed procedure of the review process is also available in this publication [60].

From recent narrative review papers on genotoxicity, it appears that results are mainly inconsistent, and the effects, when present, are a function of frequency, amplitude, and modulation, and in most cases are not replicated in follow-up studies [61][62][63][64].

Most of these review papers also highlight the importance of the methodological quality of the experimental studies. Thus, in order to consider the available genotoxicity results concerning exposure to RF-EMF, it is important to check whether quality control measures were included in the experiments, as the absence of the latter introduces a methodological bias. In the review by Vijayalaxmi and Prihoda [65], the percentages of publications reporting no significant difference in genetic damage between RF-exposed and control cells were positively correlated with the increase in the number of quality control measures/scores adopted in the investigations. Moreover, the comprehensive review of quality assessment made in this study also revealed that when exposure to RF energy was at a SAR level above the ICNIRP guidelines, there was increased damage due to a thermal phenomenon or due to the presence of highly localized hot spots. The same authors showed using a meta-analysis approach that the mean indices for chromosome aberration, micronuclei, and sister-chromatid exchanges in RF-exposed and sham-exposed/unexposed controls were within the spontaneous levels reported in a large database. Studies published from 1990 to 2011 addressing genetic damage in animal and human cells exposed *in vitro* to RF-EMF were included in that meta-analysis [66]. A systematic review coming out in the next months will evaluate the associations between the exposure to RF-EMF and genotoxicity in *in vitro* experimental models. The protocol, presenting the detailed procedure of the review process, has been recently published in Elsevier's Environment [67].

In the narrative review co-authored by Wood and Karipidis [28], several *in vitro* and *in vivo* papers dealing with the effect of RF-EMF exposure on Ca^{2+} levels have been analysed. The authors computed the Effect Size (ES) defined as the difference between the means of the exposed and sham groups divided by the standard deviation of the sham group. Moreover, they assigned a quality score to each paper based on the attention given to aspects like dosimetry, sham control, positive controls and blinding. In 60% of the analysed papers, a change in intracellular calcium was reported with the number of papers reporting an increase approximately equal to the papers reporting decrease. The greatest proportion (40%) reported no changes. Analysis of ES vs. carrier frequency and modulation type did not evidence any significant relationship. The majority of the studies with a higher quality score did not report an effect. There was no consistent evidence of power density or SAR windows although the authors pointed out that estimation of exposure is to be used with caution since, in some cases, the procedure for exposure levels is not clearly described. Moreover, they evidenced that the direction of the effect moved from cytoplasmic loss to cytoplasmic gain as methods for estimating calcium levels have become more sophisticated. The papers in which the voltage-gated calcium channels (VGCCs) were investigated by direct measurement of cellular Ca^{2+} current are particularly interesting since such channels have been suspected to be susceptible to RF-EMF due to the coupling of RF-EMF to cells and the demodulation of extremely low-frequency modulations from the RF-EMF carrier [68][69]. These papers did not show significant effect due to RF exposure and thus did not support the claim that VGCCs are particularly sensitive to environmental RF-EMF exposure. Based on the overall results of these reviews, the authors concluded that future good quality experiments are needed to support the claim that calcium levels are affected by RF exposure. The systematic review by Bertagna et al. [70] analysed the effects of EMF on neuronal ion channels. They collected papers published in the years 2005-2020 and found that 33% of the total papers covered RF-EMF. The RF papers did not show significant effects after acute exposure while effects were reported under chronic exposure. However, detailed description and reproducibility of the exposure parameters (dosimetry) are a basic requirement for evaluating the quality of evidence used for risk assessment. It appears that several studies on RF-EMF effects included in the above systematic review did not meet this requirement.

Recently, Romeo and co-workers performed a scoping review of the literature studies investigating the effects of RF-EMF exposure on the apoptotic process, with the aim to systematically mapping the research performed in this area and identifying knowledge gaps [71]. A systematic literature search was performed; 121 potentially relevant studies were retrieved, but only 42 complied with basic quality criteria (adequate characterization of exposure conditions, appropriate dosimetry, presence of sham control, temperature monitoring, a minimum of three independent experiments performed) and were included in the analysis. Most of the included studies did not find any significant impact of RF-EMF exposure on the apoptotic process. When a statistically significant effect was observed, it mainly occurred at frequencies above 6 GHz, and for acute (<1h) exposure durations.

2.2.2 Red blood cells and their components as a model to study mechanisms of interaction between RF-EMF and biological systems.

Within the task 4.1 we explore whether RF-EMF exposure may elicit acute effects within minutes-to-an hour scale (duration of a phone call) on subcellular structures (plasma membrane and transmembrane proteins, cytosolic components) and intact cells. We have chosen RBCs as a model system to study the possible alterations in the protein structure and function as well as on water and protons, for the following reasons.

- These cells lack protein synthetic machinery, and we cannot expect any replacement of the damaged or altered proteins by way of de novo protein synthesis.
- RBCs do not have mitochondria, and we can thus eliminate the effects associated with mitochondrial responses to the RF-EMF irradiation.
- When in circulation, RBCs are exposed to the EMF when passing through the skin capillary circuit.
- RBCs can be easily harvested and tested for their responses to the RF-EMF after the humans are exposed to the EMF.
- Hemoglobin is a well-characterised and easily available protein, and it may be used to investigate protein responses to the RF-EMF
- We know a lot about metabolism and redox maintenance in these cells. Ion transporters in human RBC membrane are relatively well characterised.
- RBCs possess NO synthases and, hence, NO production may be studied in intact cells.

Listed below are methodological approaches and techniques we have chosen to assess the possible effects of EMF on RBCs and their components.

Intracellular free and bound water: Water molecules are the major targets of microwave EMF. Peak of absorbance for water is within the RF-EMF frequency range. Hydration of proteins, ions and other molecules in the cytosol may reflect the changes in their structure [17]. The changes in hydration shells of biomolecules are assessed by HUJI partner using dielectric spectroscopy [16][72].

Hemoglobin: Exposure of hemoglobin in aqueous solutions was shown to respond to EMF exposure with structural changes which may result in the alterations in O₂ affinity to the hemes [73]. Heme-containing proteins respond to magnetic field when heme iron is in ferrous deoxygenated or carboxylated state or when in ferric state as in met-hemoglobin (metHb) or hemichromes [74][75].

Tumbling and redistribution of the surface charge of proteins exposed to RF-EMF due to the shifts in dissociation constants may result in the changes in times spent in different conformations. These changes in protein dynamics may be resolved using different experimental techniques. So far, circular dichroism assessment of protein conformation in aqueous solutions of purified proteins failed to provide evidence for conformational responses of the thermosensory protein GrpE of the Hsp70 chaperone to exposure to 0.1, 1, or 1.9 GHz EMF with or without modulation [76]. However, changes in O₂ affinity and spectral characteristics of Hb were reported after exposure of Hb solution to 0.91 and 0.94 GHz [73] suggesting the induction of conformational changes by RF-EMF.

We are planning to apply several approaches to assess the effects of EMF exposure on Hb conformation. Hb is a strong buffer, and conformational changes are highly likely associated with the changes in the pK of the protein. Solutions of freshly prepared oxyhemoglobin from human RBCs will be prepared in unbuffered solution, and the pH of the solution, which is defined by the state of Hb, will be monitored in sham and EMF-exposed samples as a function of RF-EMF exposure time. This experiment will be performed with oxy-, deoxy-, and met-Hb as well as for oxygenated and deoxygenated intact RBC suspension in isotonic unbuffered medium. Co-oximetry will be performed using EDAN I20 blood gas analyzer, Diatools AG.

Intraerythrocytic free Ca²⁺ levels: Based on the earlier reports of other research groups we consider that Ca²⁺ transport systems (channels and/or Ca²⁺ ATPase) across the RBC membrane [77] could be molecular targets of RF-EMF. As the steady-state levels of free Ca²⁺ in RBC is temperature-dependent (see below), it is important to assess if the effects are thermal or non-thermal or mixed. It is also important to identify the molecular mechanisms involved in the observed effects. RBCs membranes possess a number of Ca²⁺-permeable cation channels and a plasma membrane Ca²⁺ ATPase (PMCA) [78][79]. Among the channels that were studied for their sensitivity to RF-EMF exposure by other groups [28], RBCs may serve as a model to explore potential effects on transient potential receptor channels (TRPC2,3,6), Piezo1 channels, transient potential vanilloid receptors TRPV, voltage-gated cation channels and N-methyl D-aspartate (NMDA) receptors [79]. Among the experimental techniques that may be used to study the activity of these channels we favour fluorescent imaging techniques (Flow cytometry and

microscopy) using fluo-4 AM (for the reasons see [80]) as a fluorochrome of choice as they may be acquired to the cells immediately after exposure to the microwave EMF. Recent advances in automated patch clamp technologies make it possible to perform electrophysiological recordings on 384 cells (at best) at the same time using Nanion's SyncroPatch devices [81], but this approach cannot be used immediately following exposure to EMF.

Intracellular Na^+ / K^+ levels: A mechanism proposed for the action of EMF on ion channels (voltage-gated and mechano-sensitive) implies that the vibration of the inorganic ions forces by the EMF alter their passage through the channel pores, interaction with the ion channel gates and with the modulators such as Ca-calmodulin, and with the channel environment (lipids and sugar moieties) [31][33]. The physics and chemistry of the effects of RF-EMF on the membrane proteins reported by several groups remain to be clarified. Impact on the ion channels [33] and $\text{Na},\text{K}\text{-ATPase}$ [26][49][50] were reported. Marino et al. [51] have explored the four possible types of ion channel-based "EMF-sensors", which could respond to the force, light, chemical stimulation, or the movement of negatively charged sugar chains attached to the extracellular domains of the ion channels in response to the EMF exposure. Monitoring of evoked potentials in the brain of exposed persons suggested that the EMF receptor channel is most likely a mechano-sensitive receptor reacting to the force [51]. Changes in the opening probability of ion channels in response to irradiation, an effect which is utilized for pain management [54]. Structural changes in the cytoskeleton in intact cells were also reported in response to RF-EMF exposure [55]. Movements of Na^+ and K^+ across the RBC membrane may be visualised directly (by monitoring the changes in Na^+ in the extracellular medium or in the cells using ion-selective electrodes of flame photometry [82][83][84][85]. Our recent experiments revealed that massive Na^+ uptake by RBCs may also be detected at the single-cell level using CoroNa Green fluorescent dye [86].

Cellular deformability and osmotic stability: Changes in ion content in RBCs is associated with shrinkage/dehydration following net $\text{K}^+\text{-Cl}^-$ loss from the cells or swelling/overhydration following $\text{Na}^+\text{-Cl}^-$ uptake. Uptake or loss of water and volume alterations, in turn, result in the changes in deformability and ability to resist hyperosmotic or hypoosmotic stresses. Together with the changes in hydration, changes in red blood cell deformability may originate from the loss of membrane as a result of vesicle release or from the loss of elasticity of proteins forming cytoskeleton (reviewed in [87]). On the contrary mild oxidative stress does not alter cell volume in human RBCs (Busch and Bogdanova, unpublished), while strong oxidation decreases the deformability and reduces lateral membrane mobility (tank-treading) [88]. The deformability of RBCs is explored using LoRRca MaxSis analyser in the osmoscan and deformability modes [89]. Single-cell measurements are performed using a cell-flow analyzer [90].

Aggregability: Exposure to RF-EMF was also reported to increase the aggregability of RBCs and promote the formation of stacks of cells known as "rouleaux" aggregates [91]. The exact molecular mechanism of rouleaux formation upon RF-EMF exposure is not known. It was proposed that staggering of exposed RBCs is induced by the "pearl-chain effect" (i.e., the aggregation or lining-up of dielectric particles in a fluid, resulting from attractive forces between), or via impacting the negative charges at the glycocalyx of the membranes. Under the influence of RF electric fields, electrical charges tend to accumulate on opposite cell surfaces to form induced dipoles, whose orientation changes with oscillations of the field. Dipole–dipole attractive forces occur in the process, which are enhanced when the cells are near each other. The dipoles then align in the direction of the applied electric field and form chains of many cells or molecules. This effect has been observed under RF electric fields at frequencies up to 100 MHz [12]. Erythrocyte sedimentation rate will be used as a measure of aggregability along with microscopic examination of the aggregate formation.

3 New EMF exposure setups for red blood cells in flow

Detailed information on the specifications of the new exposure setup will be provided in deliverable D4.7.

Engineering teams and physicists from HUJI, TUD, UNICAS and THUAS were joining forces to develop the optimal exposure conditions for blood, RBCs and cell components that would imitate far-field exposure.

The initial setup was based on a thermostabilized exposure cuvette with plate electrodes immersed in the liquid under test as a source of EMF, as depicted in D4.1. Such a near-field configuration was not satisfactory in terms of uniformity of the field distribution inside the sample; in addition, the unbalanced feeding network made the numerical dosimetry not fully reliable. Consequently, a new exposure setup has been designed to allow exposure in far-field conditions.

3.1 Exposure setup for the far-field mode of exposure to the RF-EMF of 3.5 GHz

The selection of real signal features, as well as exposure conditions involving flowing blood aims at assessing real-life exposure. This is one of the main objectives of the NextGEM project, and specifically of Case Study 2 and Case Study 3 investigating effects of the 5G FR1 and FR2 bands, respectively. In the framework of case studies, simulations will be carried out to model both indoor and outdoor exposure scenarios, as well as measurements in real environments, in order to identify the main exposure features to be used with the proposed exposure setup to investigate possible biophysical and biochemical mechanisms on RBCs. A new prototype was designed fitting these requirements. In this setup, the antenna is located above the sample and the distance between the antenna and the thermostated blood sample may be adjusted to fulfil the far-field condition. Numerical dosimetry was performed by the HUJI partners using simulations resulting in the following setup dimensions (see Figure 1, Figure 2 and Figure 3).

3.1.1 Equipment and Materials

The EMF exposure system consists of the following components:

- RF Generator (Agilent E4438C Vector Signal Generator)
- RF Line (35 cm Coaxial Rigid Cable 50 Ohm, N-N connectors)
- Antenna (UWB Inverted T-slot patch antenna, 2 dBi, 1.24 VSWR at 3.5 GHz)
- Thermostabilized 3D printed cuvette for circulated biological fluid (such as blood, RBC suspension, proteins solution, etc.) for EMF exposure (see Figure 1).
- Peristaltic pumps
- Silicon tubes for biological fluids circulation
- The oil-based-heat circulatory system Julabo CF41
- The thermocouple

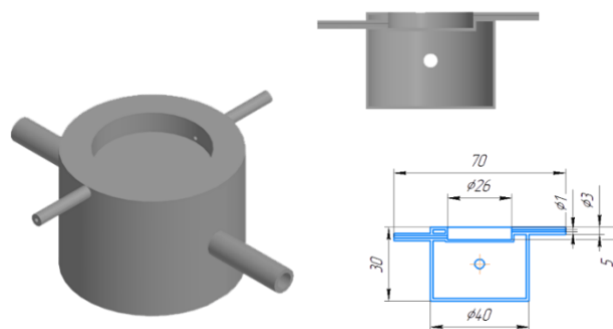


Figure 1: Far-Field EMF Exposure Cell (3D printed), dimensions shown are in mm.

The antenna and the exposure cuvette (Figure 1) are placed into a protective case coated inside with absorbent material (~ 30 dB) to minimize losses and external influence of electromagnetic fields (Figure 2). All additional installation elements (such as a generator, circulator, experimental cuvette, etc.) will be outside the shielded box.

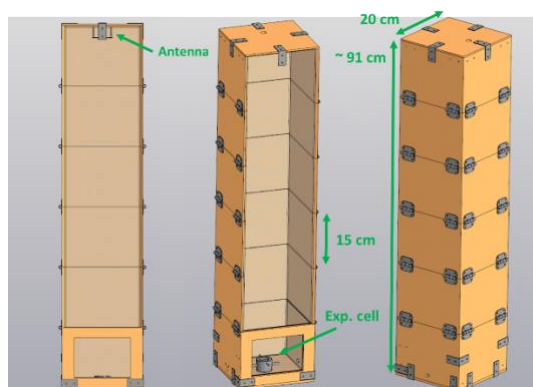
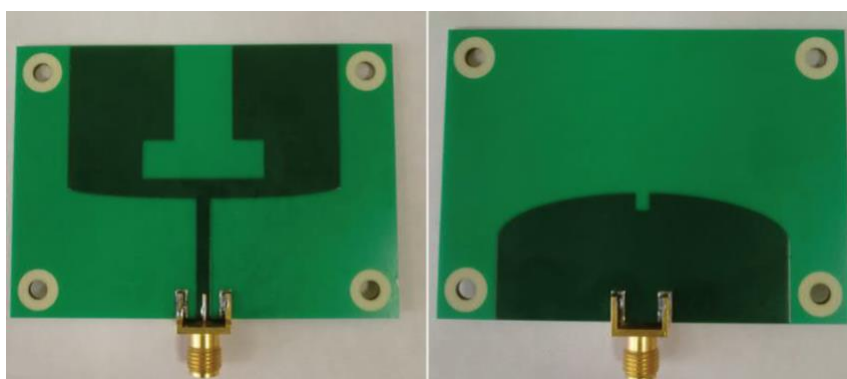


Figure 2: Scheme of the protective cover with dimensions set for the 3.5 GHz frequency.

An inverted T-slot bidirectional ultra-wide band patch antenna was used for the pilot experiments, which fully satisfies the study requirements. This type of antenna was detailed elsewhere [92]. The antenna was modified but its basic parameters were preserved. In FR2 a similar design will be developed, or a horn antenna will be selected.

Figure 3a shows the physical appearance of the antenna used in experiments and Figure 3b shows its geometry for modeling and manufacturing.

A



B

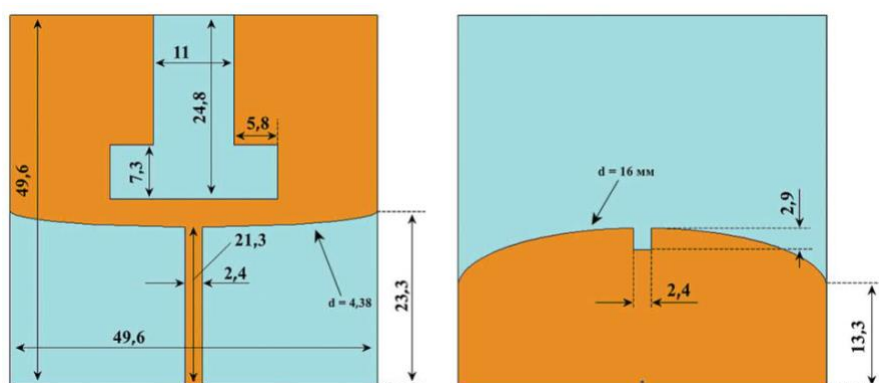
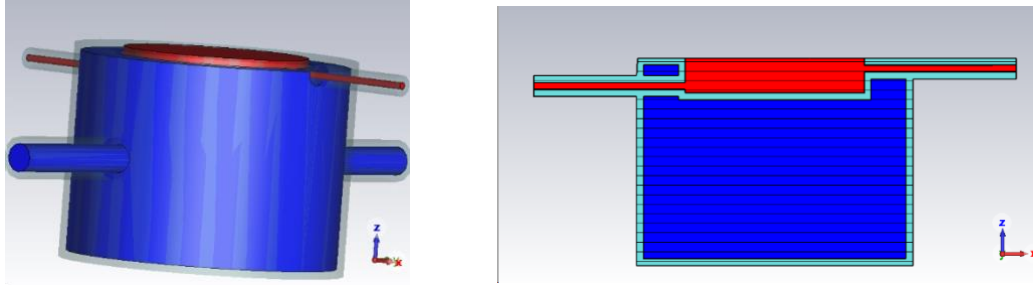


Figure 3: Physical (A) and schematic representation of the antenna (A) top and bottom views; (B) antenna's geometry.

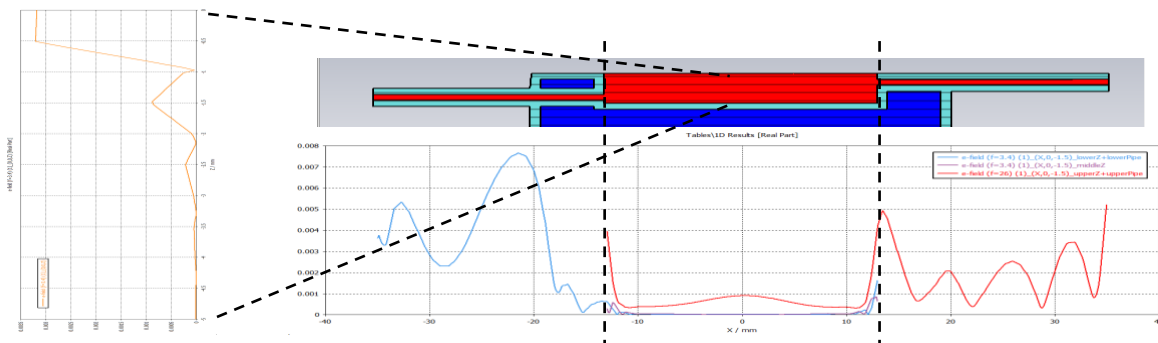
This type of antenna was studied in detail and optimized in CAD.

We optimized the construction of the exposure cuvette by simulating the distribution of the EMF (Figure 4a). The simulation, carried out by means of the software CST Microwave Studio, was performed for fields of two frequencies: 3.5 GHz (Figure 4b) and 26 GHz (Figure 4c).

A



B



C

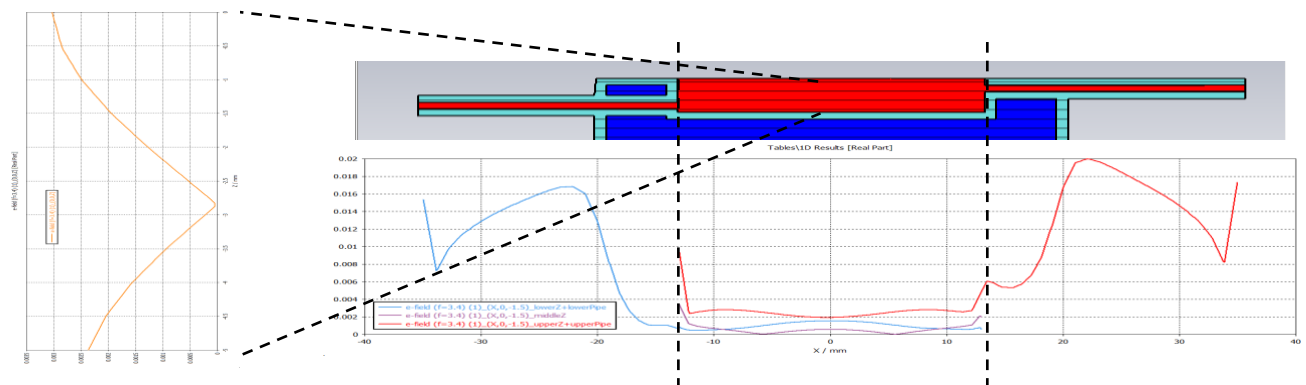
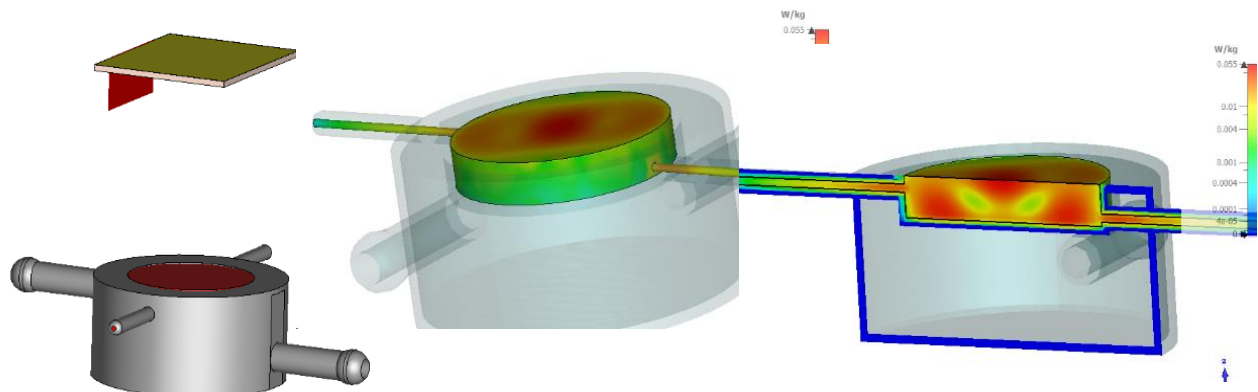


Figure 4: CST simulation for the exposure cuvette (A), CST Simulation of the plane-wave ~3.5 GHz, distance between the antenna and the sample's brim is 4λ (B) and simulation of the plane-wave 26 GHz, distance between the antenna and the sample's brim is fixed at 4λ (C).

The simulated SAR at 3.5 GHz is presented in Figure 5a. The left panel shows the visualization of the simulation setup – the cuvette filled with blood at 37 °C with patch antenna located at 4λ distance above the blood sample brim. The central and right panel show the top and side views of the power distribution in the sample. The same power density visualization for the 26 GHz is presented in Figure 5b.

A



B

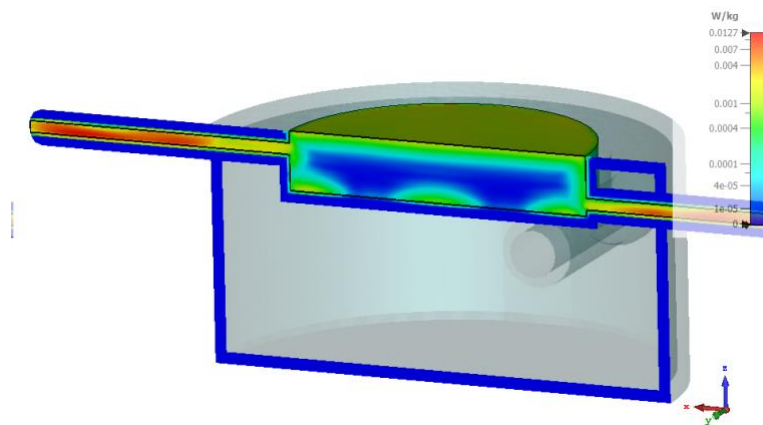


Figure 5: SAR distribution in the blood sample based on the CST simulation for the 3.5 GHz (A) and the 26 GHz (B). (A): On the left – the simulation setup. The cuvette filled with blood at 37 °C with patch antenna located at 4λ distance above the blood sample brim. The middle and right panels represent the SAR distribution in the sample, top-side view and a cut-side view, respectively. (B): SAR distribution at 26 GHz with a plane wave source, located at a distance of 4λ . We used the Microwave Dielectric Spectroscopy method to control the EMF exposure effect.

For 26 GHz we have used a plane wave source. Figure 5b shows the SAR distribution in the blood sample. The numerical dosimetry will be thoroughly reported in deliverable D4.7, together with the finalized design of the exposure setup.

3.2 Unified signal to expose biological samples and the generator/interface to produce it

Within the NextGEM project, exposure of cells (RBC, human lymphocytes, human keratinocytes (HaCaT), neuroblastoma cell line (SH-SY5Y)), a small organism (*C. elegans*) and healthy human volunteers are foreseen. Moreover, based on the results obtained for the exposure of human volunteers to RF-EMF fields in emulated and real conditions, different measurement campaigns will be carried out. In order to be able to compare the responses to the pulsed RF-EMF obtained by the project partners, the NextGEM consortium decided to harmonize as much as possible the stimulus to be used in the different experiments, taking into account the different available hardware (HW).

Our choice of the unified pattern of signal is based on the concept of RF modulated signals, as they are used in modern telecommunication systems. Information transfer in a wireless channel starts with coding of the digital bit

stream (information). The obtained coded signal is then superimposed on a high frequency carrier (i.e., 3.5 GHz and 26.5 GHz for the case of 5G). The resulting merged signal is an amplitude and phase modulated wave that can be transmitted on a wireless channel using antenna interfaces, as shown in a simplified version in Figure 6b, compared to the simple pulsed signal plotted in Figure 6a.

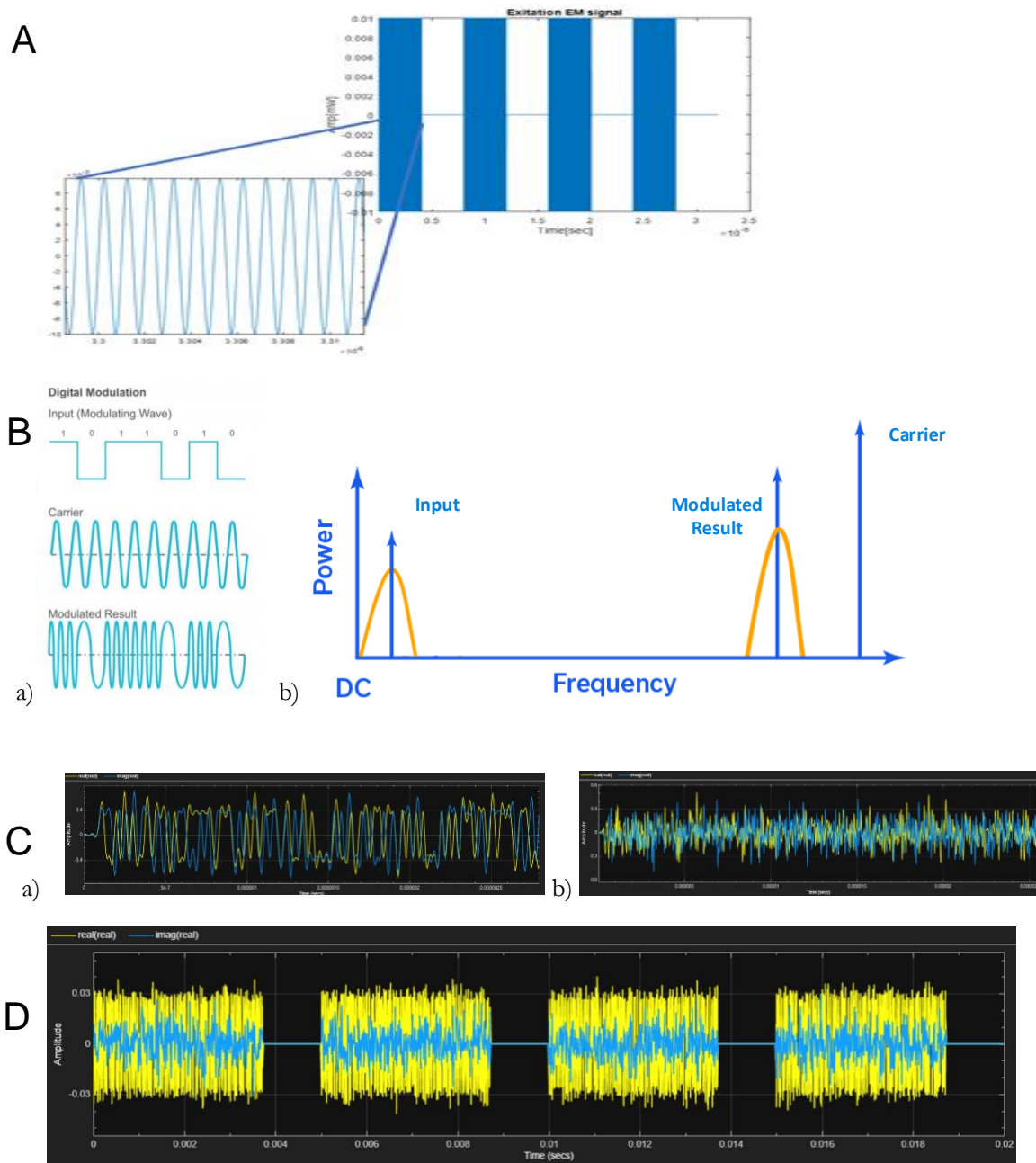


Figure 6: Signals temporarily used and the unified signal to be used in the future in the biological experiments. (A) The signal used for RBC sample is a squared pulse, modulated with the sinus of the 900MHz, 1GHz and 3.5GHz. The pulse width of 100 microsec and the duty cycle of 10% was used. The signal power was 10dBm at the output of the signal generator port. (B) RF modulation (simplified) concept, described in the (Ba) time domain and (Bb) frequency domain. (C) I and Q waveform of data modulated using a QAM (Ca) and an OFDM modulation (Cb). (D) I and Q time domain waveform of 5G NR test model 3.1.

RF synthesizer can very accurately set the frequency of the high-frequency carrier with high precision (i.e., hundredths of hertz precision). Nevertheless, as mentioned above, the time fluctuation of the high-frequency (modulated) signal will be defined by the input (baseband) content.

In addition to the specific data content, the modulation type (i.e., the specific mapping from bit to waveform) plays a significant role in the signal dynamic, as can be seen in Figure 6c, where the same data is modulated on the high

frequency carrier using different modulation types and the I and Q time domain waveforms are shown, QAM and OFDM, Ca) and Cb) respectively.

Finally, when the same QAM modulation is applied and a standard 5G signal protocol is applied, (i.e., mapping the synch signals and the various physical and paging channels), the signal dynamics over which the frequency carrier is modulated are yet again strongly different, as can be seen in Figure 6d.

After gathering the information on signal generator hardware capabilities from the various groups, the NextGEM consortium decided to define a 5G NR baseband signal, which would mimic a time slice of a signal used in real life, which can be used in all the different experiments.

The high-level signal information is summarized in the Table 2. For more details on the meaning of the parameters see Deliverable D2.2. The baseband signal has been generated by the University of Cassino and Southern Lazio and made available to all the partners to be employed in their future experiments. All the parameters are chosen to comply with the 5G standard¹ (see D2.2), but some choices could be changed since they are related to the HW to be used and to the scenario modelling, which are currently under definition. The proposed approach will ensure a higher level of uniformity for the biological experiments performed at the NextGEM partners' sites, allowing to compare the results obtained in the various experiments and case studies. In addition, the chosen parameters will also allow the extension of the comparison with analogous studies carried out within the other projects funded by the EU in the framework of the Clue-H cluster.

Table 2: Unified signal characteristics

Parameters	Characteristics
PAPR	12 dB
Duplex mode	TDD
Waveform format	DFT-s-OFDM
Modulation scheme	QPSK
Subcarrier spacing	30 kHz in FR1 (3.5 GHz), 120 kHz in FR2 (26.5 GHz)
Channel bandwidth	100 MHz (50 MHz in case of HW limitations)
% of RBs	100% RBs
Signal duration	20 msec
TDD	75%

¹ In particular, test models NR-FR1-TM1.1 and NR-FR2-TM1.1 have been selected in the two bands, as defined in TS 38.141-1 and TS 38.141-2, respectively. A few parameters have been changed according to Table 2.

4 Temperature-dependence of the parameters of interest

Most of our knowledge on the mechanisms of interaction between the microwave EMF and the biological systems is on the thermal effects which arise from absorbance of the energy of EMF by water, as explained in the Section 2.1. While the thermal effects of the EMF on cells and tissues are not questioned, the existence of nonthermal effects is disputed. To assess the contribution of the thermal component in our responses at higher signal power densities, we have performed experiments on the possible effects of temperature on the parameters we test for responsiveness to the EMF.

4.1 Kinetics of thiol-disulfide exchange reaction between the oxidised glutathione (GSSG) and reduced thiols of hemoglobin molecule

4.1.1 Introduction

Non-enzymatic reaction between the GSSG and SH-groups of cysteines within the α and β globin chains of hemoglobin occurs only when sulfide is in the dissociated form and is accessible for GSSG to approach it. The resulting product, S-glutathionylated GSS-P adduct, is stable and its de-glutathionylation requires enzymatic catalysis. We hypothesized that, when occurring, the transient short-lived changes in hemoglobin structure caused by EMF exposure may be visualised through the alterations in thiol disulfide exchange reaction and preserved for analysis as the reaction product is stable.

Interaction of deprotonated SH-groups of proteins with oxidised glutathione is known as thiol-disulfide exchange and results in production of S-glutathionylated adducts:

Protein-S⁻ + H⁺ + GSSG (oxidized glutathione) = Protein-SSG (S-glutathionylated adduct) + GSH (reduced glutathione)

Regeneration of Protein -SH from S-glutathionylated form may occur in reaction catalyzed by an enzyme, the glutaredoxin [93][94]. This protein modification is triggered by oxidative stress. Apart of GSSG which accumulates in the cell in response to oxidation, S-glutathionylation may be triggered by mild oxidative stress that transfers SH-groups to thiyl radical -S[•] or -SO[•] (sulfenic acid), both of which may interact with reduced glutathione GSH. Being reversible, S-glutathionylation prevents irreversible oxidation such as sulfinic (P-SO₂) and sulfonic (P-SO₃) acids

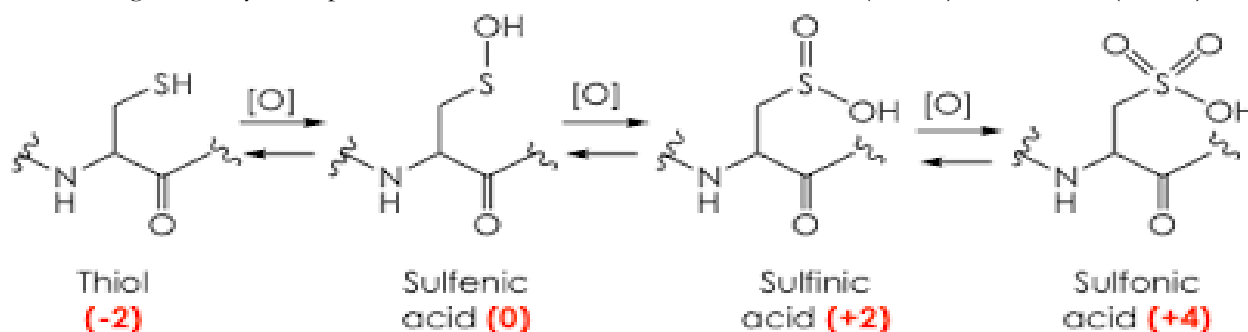


(Fig. 7).

Figure 7: A sequence of thiol oxidation steps where sulfur (S) changes its oxidation state from -2 to +4.

When irreversible oxidation of SH-groups takes place, protein is degraded and replaced by a newly produced one in all cells that are capable of *de novo* protein synthesis [95]. Mammalian RBCs are not producing new proteins, they lack nucleus and protein synthesis machinery. Therefore, RBCs that accumulate terminally oxidized proteins are removed and replaced by new cells. S-glutathionylation in RBCs thus protects these cells from premature clearance. One more function of S-glutathionylation is the impact of glutathione binding to the protein-on-protein structure and function [93][94][96][97][98].

Dissociation of thiols of thioredoxin was suggested to be affected by EMF irradiation and is claimed to represent a non-thermal effect of it [99].

Adult human Hb (HbA) tetramer consists of two alpha and two beta-globin chains containing all together 6 cysteines (two of the following cysteines: Cys93B, Cys112B and Cys 104A) per tetramer (more on that in D4.1). Each cysteine contains one thiol group that may be S-glutathionylated, but they have different reactivity [100] and different kinetics for S-glutathionylation of different groups may be expected. Increase in S-glutathionylation of HbA has been reported for smokers and patients with diabetes and is associated with changes in HbA oxygen

affinity. Furthermore, HbA thiols function as scavengers of oxidants originating from the peripheral tissues. Induction of S-glutathionylation increases O₂ affinity of HbA and compromises O₂ release in hypoxic peripheral tissues such as the heart and the brain [101][102][103]. Increase in S-glutathionylation of HbA was reported in patients with diabetes [104], those under dialysis [105], and in smokers [106].

4.1.2 Experimental procedures

Using the first near-field RF-EMF prototype of the exposure system we have observed reduction in the reaction rate of S-glutathionylation if the substrates (GSSG and hemoglobin) were exposed to a modulated 3.5 GHz signal (10 dBm) for 20 min at room temperature. Reaction kinetics remained unaltered if the modulation was omitted. As this exposure system did not meet the far-field EMF requirements, this experiment will be repeated using the exposure setup described in the Section 3.

We explored the temperature-dependence of kinetics of this thiol-disulfide reaction. We monitored the rate of accumulation of S-glutathionylated adducts of Hb when hemolysates were exposed to GSSG at 2, 25 and 37°C.

The following experimental protocol was used:

RBCs of healthy donor was hemolyzed by mixing with an equal volume of water in the presence of 1mM EDTA and a protease inhibitor mixture. Membranes were sedimented by centrifugation and concentration of oxyhemoglobin was determined using the Drabkin reagent. A stock solution of oxidised glutathione GSSG of 420 mM was prepared. The Hemolysate was pre-exposed to 2°C, 25°C or 37°C until it reached the desired temperature and then thiol-disulfide exchange reaction was initiated by adding GSSG (1:10 proportion to Hb). The reaction was stopped by adding N-ethyl maleimide (25mM) to the reaction mixture to alkylate all the free reduced thiol groups.

Thereafter, the abundance of S-glutathionylated hemoglobin was tested using immunoblotting. After protein separation on the 12% agarose gel, the proteins were transferred to the 0.45 µm Nitrocellulose membrane (Amersham Protran), and the efficacy of transfer was controlled with Ponceau Red staining. The antibodies that were used to visualise S-glutathionylated hemoglobin was detected with mouse Anti-Glutathione antibody (abcam; ab19534, 1:1000 dilution) as well as with Hb beta-chain specific Rabbit HbB antibody (abcam; ab214049 1:2000 dilution). Images of the blots were obtained using BIO-RAD ChemiDoc imaging system and densitometric analysis was performed using ImageJ software. Hb samples obtained from the cells treated with diamide catalyzing S-glutathionylation were used as positive control, while lysates treated with 10 mM DTT was used as a negative control. Mass spectrometry was used to confirm the results of immunoblotting.

4.1.3 Results and discussion

An increase in the production rate of S-glutathionylated Hb adducts in thiol-disulfide exchange reaction with GSSG with increasing temperature was observed (see Figure 8). The effect becomes visible from the first minutes of interaction between GSSG and the thiol groups of Hb if the reaction is allowed to occur at 2°C or 40°C. The differences in GSS-Hb production between 25°C and 40°C reach significance after 40 min of incubation (Figure 8). This observation is particularly important as our earlier preliminary/unpublished findings revealed that exposure to the microwave modulated EMF in near-field slows down this reaction. If this observation will be reproduced in the far-field settings, it will allow us to suggest that not all effects of RF-EMF that we observe at the molecular level are due to the temperature changes that are controlled by the ICNIRP regulation standards.

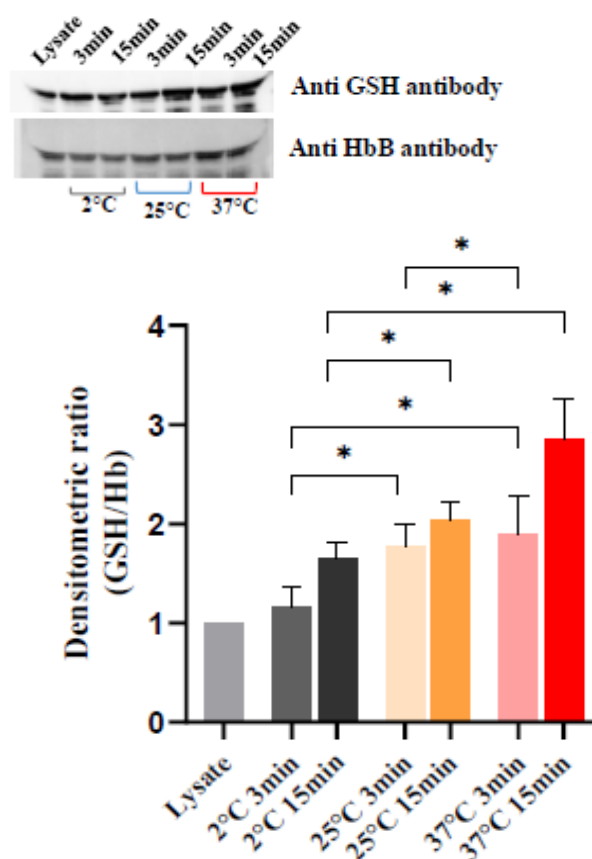


Figure 8: Temperature-dependence of S-glutathionylation of hemoglobin. The abundance of S-glutathionylated adducts is shown after 3 or 15 min of incubation of hemolysate with GSSG at 2, 25 or 37°C. Presented are the examples of immunoblots and the outcome of densitometry normalized to the Hb loading control. “Lysate” stands for the basal S-glutathionylation of Hb before the addition of GSSG. * denotes $p < 0.05$ in One-way Anova on repeated measures. Data are results of 3 independent experiments \pm SD.

4.2 Effect of temperature on the intraerythrocytic Ca^{2+} levels

4.2.1 Introduction

Effects of RF-EMF, as well as that of extremely low frequency EMF, on the activity of Ca^{2+} -permeable ion channels were reported in multiple cells and tissues, being mostly studied in the brain tissue and neuroblastoma cell line [28]. The fact that both RF and ELF may produce the changes in Ca^{2+} levels, suggest that the underlying mechanisms may not only be of thermal nature, but the existence of thermal effects on the channel activity cannot be completely ruled out. Reports on the changes in Ca^{2+} uptake rate in cells and tissues exposed to the microwave EMF are contradictory and the mechanisms of possible responses of the ion channels to modulated or non-modulated signals are unknown. One recent study reveals an increase in the intracellular free Ca^{2+} in RBCs exposed to GSM 0.9 GHz or 1.8GHz signal as a result of activation of voltage-gated cation channels [77], followed by the alterations in metabolic activity and in RBC morphology. We have addressed the temperature-dependence of the intracellular free Ca^{2+} levels.

4.2.2 Methodology

Fresh-isolated RBCs were isolated from heparinised venous blood samples and washed three times with plasma-like buffer (for composition see [85]) and subsequently were loaded with Fluo-4AM for 1 h at room temperature in the dark and then exposed to one of three temperatures (Thermoshaker; Huber lab) while shaking (300rpm) for 20 or 40 min. Afterwards, intracellular Ca^{2+} was detected with flow cytometry (BC Gallios) using Ca^{2+} -dependent fluorescent signal (excitation/emission wavelengths being 488/545 nm respectively). RBCs treated with intracellular Ca^{2+} chelators (BAPTA or permeable EDTA) served as negative control, and the cells treated with Ca^{2+} ionophore or with activator of Ca^{2+} -permeable cation channel PIEZO1, Yoda1, were used as a positive

control. Shown in this section are the data for bulk RBC population (see [85][86]). The next sets of experiments will elucidate temperature-sensitivity of individual ion transport pathways such as Plasma membrane Ca^{2+} ATPase (PMCA) [86], and the following Ca^{2+} -permeable channels: PIEZO1, NMDA receptors, voltage-gated cation channels [79].

4.2.3 Results and discussion

Studies on the responsiveness of the intracellular Ca^{2+} to the changes in temperature are shown in Figure 9. An increase in temperature from 26 to 40°C results in up-regulation of Ca^{2+} levels in RBCs. This effect may be caused by one or several processes. Those include facilitated Ca^{2+} uptake via one or more of Ca^{2+} -permeable nonselective cation channels and/or suppression of the PMCA (despite the fact that PMCA was earlier on was shown to increase its transport activity with an increase in temperature [27]). At the moment, we explore if the activity of ion channels such as Piezo1 channel, NMDA receptors, TRPV and VGCC or PMCA. The example of such experiments where dynamics of Ca^{2+} uptake by the channels and extrusion by the PMCA is shown in Figure 7b,c. Yoda is used as a chemical activator of Piezo1 channel.

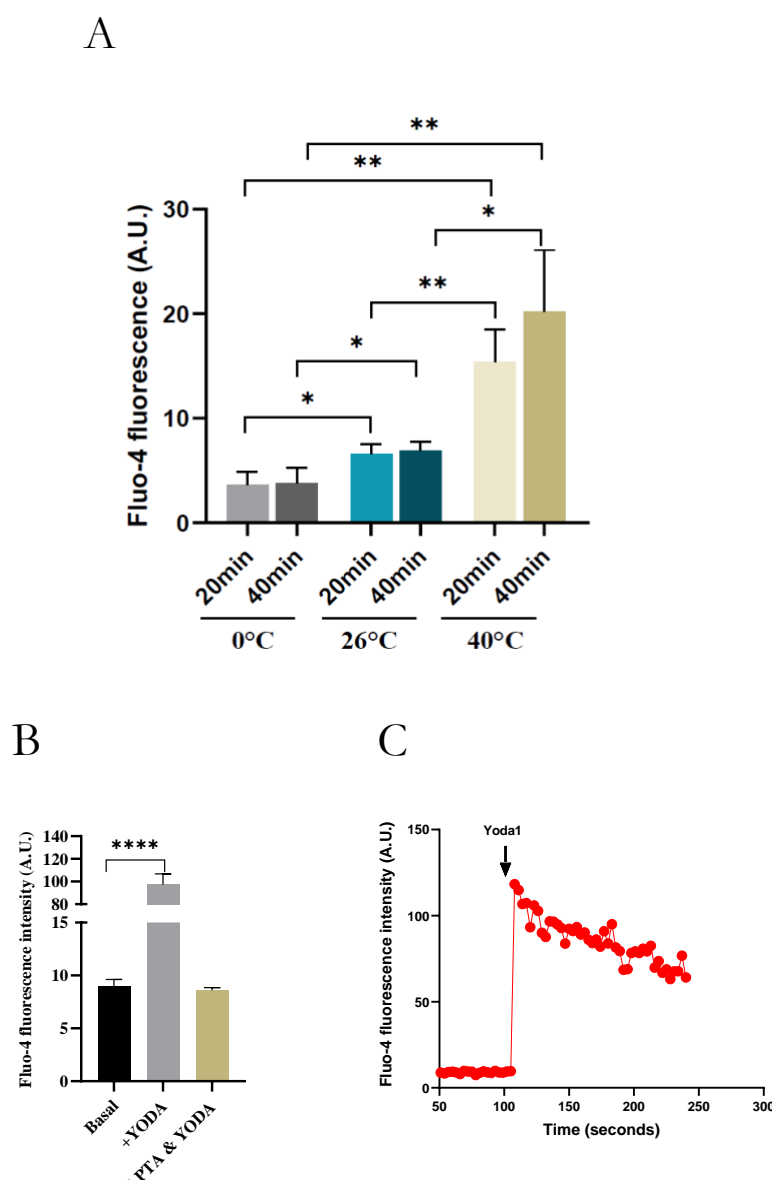


Figure 9: Temperature-dependence of intracellular free Ca^{2+} in RBCs. RBCs were incubated at designated temperature for 20 or 40 min and intracellular Ca^{2+} was then assessed by means of flow cytometry using Fluo-4 AM as a Ca^{2+} -dependent fluorescent marker. * denotes $p < 0.05$ in One-way Anova on repeated measures. Data are results of 3 independent experiments \pm SD. Shown in panel B are the negative and the positive controls. Panel C gives an example of a functional test in which the maximal activity of Piezo1 channels and the functionality of the PMCA are shown. Yoda is the activator of Piezo1 channel. BAPTA is a chelator of intracellular Ca^{2+} and serves as a negative control. Amplitude of Ca^{2+} accumulation and the kinetics of Ca^{2+} extrusion are associated with the increase or decrease in fluorescence intensity of Ca^{2+} -sensitive fluorescent dye fluo-4

4.3 Temperature effects on RBC deformability

4.3.1 Introduction

The deformability of RBCs is defined by multiple factors such as membrane surface-to-volume ratio, lipid fluidity, elasticity of membrane cytoskeletal network, hemoglobin association with the membrane, and cytosolic viscosity [87]. Some of these contributing factors are known to be temperature-dependent [23][40][107][108][109][110]. Temperature-dependence of the other contributors has not been studied in detail.

A local increase in skin temperature results in significant increase in perfusion of microvasculature (both nutritive capillaries of the elbow, and arteriovenous anastomotic capillaries at the fingertip) tested by Laser Doppler analyser [111]. Thermal stimulation of perfusion reached 300% as the skin temperature increased from 28 to 44 °C. The effects of RBC heating on their deformability were reported by several groups. Deformability was shown to depend on the temperature, magnitude of shear stress and duration of exposure [42]. An increase in temperature from 0°C to 40°C increases deformability, particularly at low shear, while further rise in temperature to 48 °C results in the ability of cells to elongate [42][112]. Matrai et al. [113] used ektacytometry to explore if exposure of RBCs to 37, 40, and 43 °C for 10 min causes the changes in the ability of cells to elongate in response to shear stress. The authors observed a significant elevation of cell rigidity, specifically under 40 and 43°C at high shear stress intensity of 30 Pa. Heating of RBCs to the lethal temperature of 48°C or more was reported to increase RBC membrane viscosity and in membrane bending resistance, doubling of membrane rigidity, along with the reduction in deformability [112].

Liu and colleagues [114] used previously obtained experimental results for the silico RBC models they developed, and came to the conclusion that RBC heating leads to the degradation of RBC deformability comparable to some disease-damaged RBCs, such as malaria. When RBCs pass through a microchannel or a slit, heated cells show longer transit or retention time. In addition, these kinetic parameters depend on the level of restriction and the heating procedure.

4.3.2 Methodology

We used two independent approaches that may be used to estimate the changes in deformability. The changes in forward scatter were used as an indirect measure of the possible alteration in RBC deformability at modest shear stress at room temperature. On the other hand, Laser optical rotational red cell analyser (Lorrca® Maxxis, RR Mechatronics) offers two ways to detect RBC deformability directly. One assay allows exposure of RBCs to a constant supra-physiologically high shear stress of 30 Pa while the cells undergo swelling or shrinkage. This technique, known as osmoscan, allows to obtain information on the membrane osmotic stability, hydration state and deformability of RBCs (for details see [87][115]). The other method is exploring deformability of cells as a function shear stress intensity at constant cell volume. Both above-mentioned assays are performed at constant temperature of 37°C. This means that the changes in rheology of RBCs measured using the Lorrca analyser will only detect the alterations that are not reversed within several minutes after the cells were transferred from the temperature at which they were incubated to the temperature at which their deformability was analysed at 37°C. Further single-cell response to an increase in temperature from 25 °C to 40°C were conducted using cell-flow analyser available at the HUJI site [116].

4.3.3 Results and discussion

As follows from Figure 10, the accumulation of Ca²⁺ was associated with a decrease in forward, but not the side scatter fitting to the changes in hydration state caused by the opening of the Ca²⁺-sensitive Gardos channels. However, these changes could not be detected as alterations in hydration state or RBC deformability at 30Pa shear stress (Figure 11). However, some trend to a decrease in elongation index while the cells were incubated at 40°C could be detected in pilot experiments where low shear stress intensities (0.3-0.5 Pa) were applied (Figure 12d), while this difference disappeared at shear stress above 0.5 Pa. As the changes in deformability observed at 0.3 Pa may reach 20% of the initial value, more experiments will be performed to resolve the possible statistical significance of this difference. Similar outcome was observed by the partners from HUJI that used their microfluidic setup that was described elsewhere [116]. Shear intensity produced in this system is also below 1 Pa.

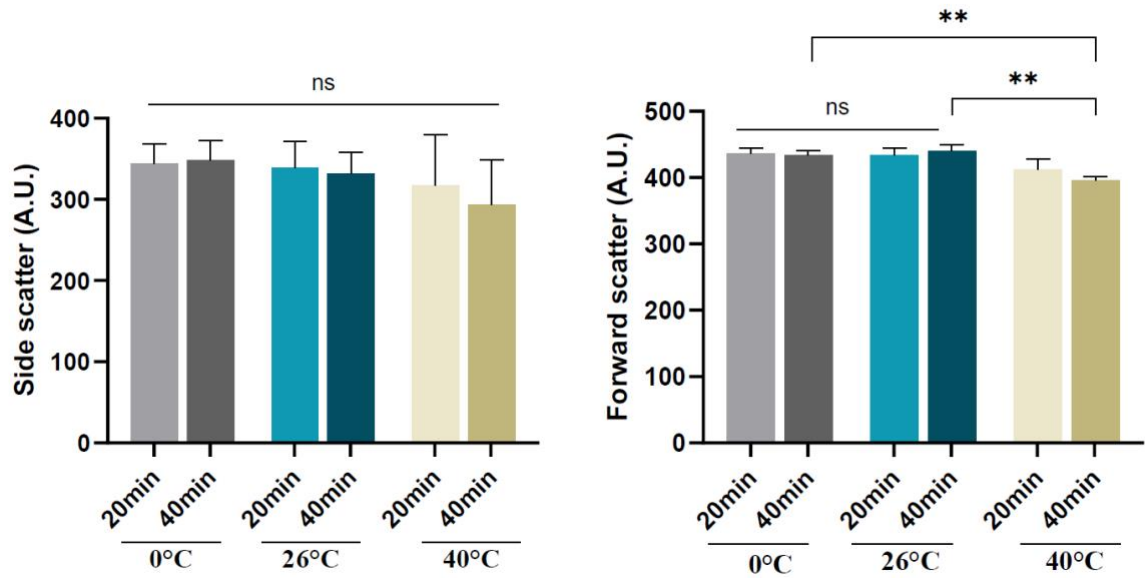


Figure 10: Temperature-dependence of forward and side scatter measured by flowcytometry. * denotes $p < 0.05$ in One-way Anova on repeated measures. Data are results of 3 independent experiments \pm SD.

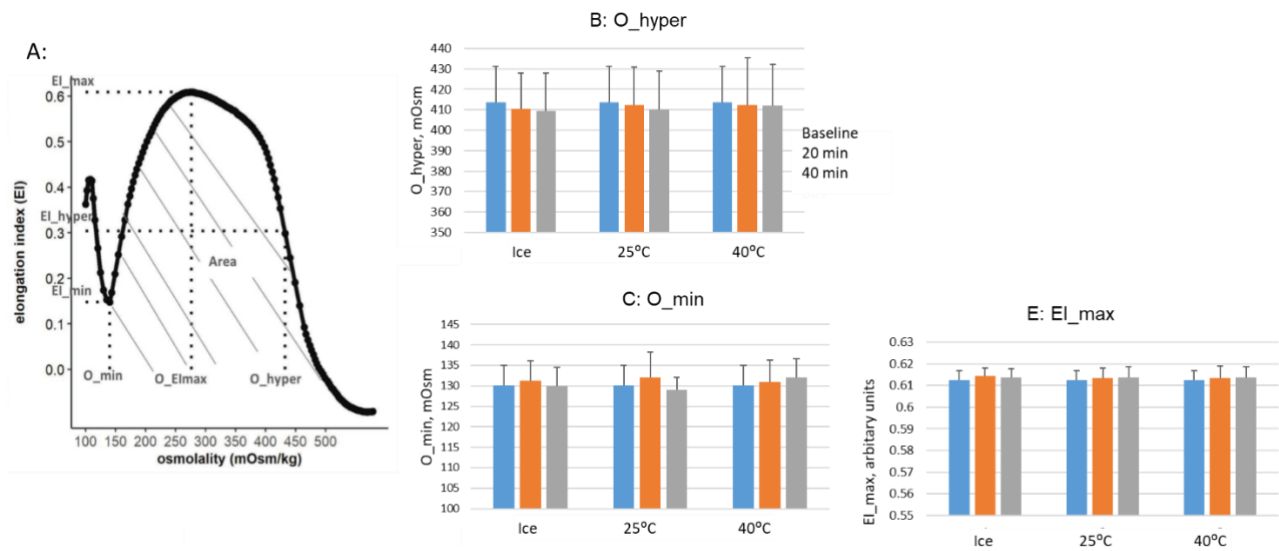


Figure 11: Temperature-dependence of the osmoscan parameters obtained using Lorrca red blood cell analyzer. Shown in the figure are half-maximal and minimal tolerated osmolarities O_{hyper} (A) and O_{min} (B) as well as optimal osmolality (O_{EImax} , C) and maximal elongation index (EI_{max} , D). Readouts obtained at the shear stress of 30 Pa. Results are means \pm SD of three independent experiments.

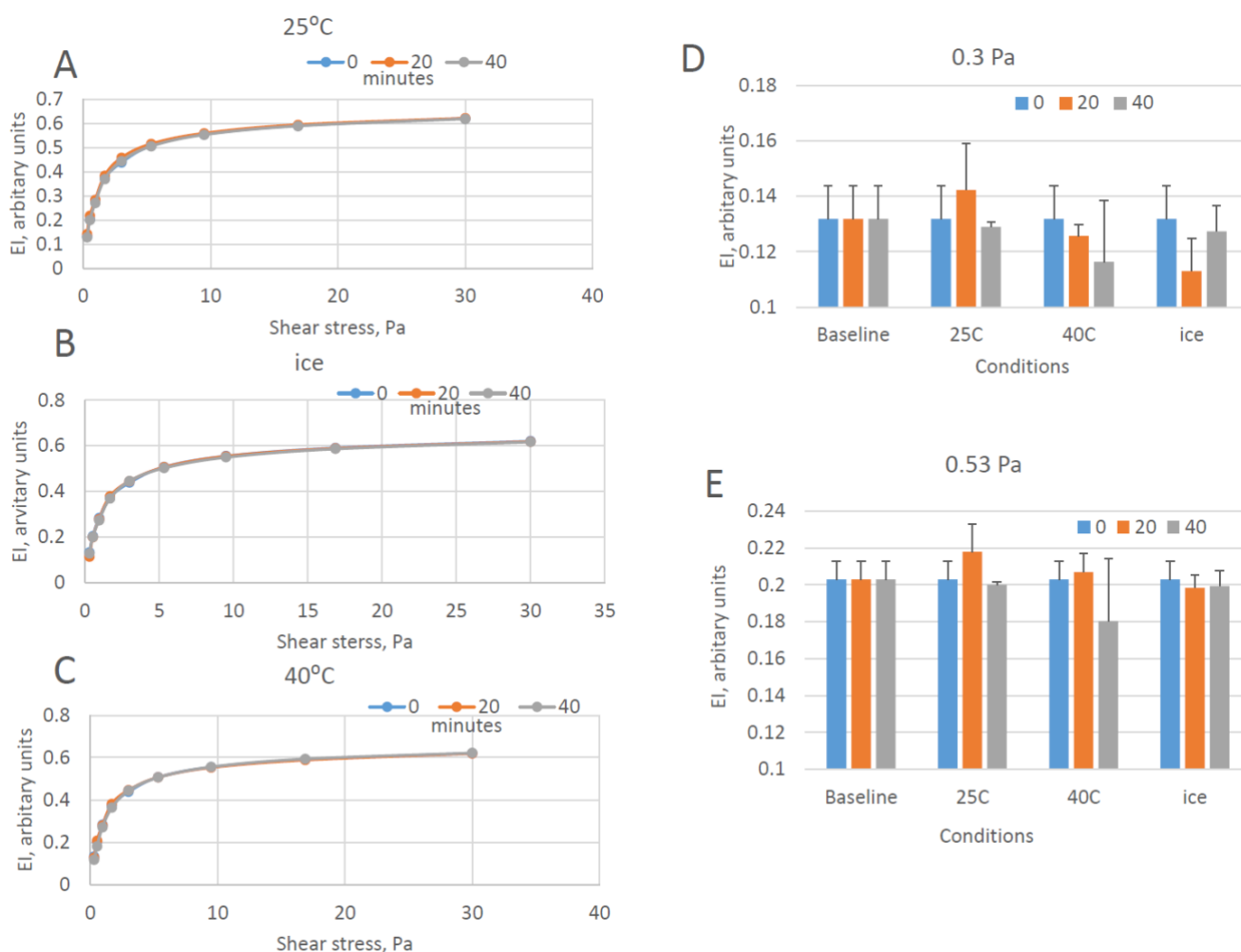


Figure 12: Temperature-dependence of RBC deformability presented as elongation index at different intensity of shear stress. Data are results of 3 independent experiments \pm SD.

The partners from HUJI have used single cell approach to study deformability (elongation index) at shear rates below 1 Pa. The whole blood (preserved with Li-heparin) of healthy donors was exposed to 40°C for 20 or 40 min. After incubation, the cells were washed in a phosphate-buffered saline and subjected to deformation measurement. Deformation was measured using a cell-flow analyzer (CFA), described in detail elsewhere [90][117].

As follows from Table 3, reduction of the elongation index, and in the medium elongation ratio (MER) of cells and an increase and percentage of low-deformable cells (%LDfC) in the population was detected. At the same time, a significant decrease in the population of high-deformable cells (%HDfC) was observed.

Table 3: Alteration of RBC deformability parameters after incubation of RBCs under 40°C (data are results of 3 independent experiments \pm SD)

Samples	MER	UDfC, %	LDfC, %	HDfC, %
Control	1.554 \pm 0.023	2.122 \pm 0.678	16.106 \pm 3.389	4.823 \pm 1.073
20 min	1.452 \pm 0.006*	3.352 \pm 0.177	26.347 \pm 0.540*	2.661 \pm 0.519*
40 min	1.435 \pm 0.029**	3.622 \pm 0.621	28.776 \pm 4.504*	2.703 \pm 0.904*

MER – median elongation ratio;

UDfC – un-deformable cells (cells with elongation ratio less than 1.1);

LDFC – low-deformable cells (cells with elongation ratio less than 1.3);

HDFC – high-deformable cells (cells with elongation ratio high than 2.5).

* denotes $p < 0.05$ and ** stands for $p < 0.01$ compared to control (exposure to room temperature, data constant for 40 min)

Taken together, these findings support a durable decrease in deformability in RBCs at low shear stresses after exposure of whole blood to 40°C.

4.4 Temperature effects on nitric oxide production by RBCs

4.4.1 Introduction

Production of nitric oxide (NO) is essential for controlling of blood pressure and the efficacy of O₂ delivery to the tissues. When produced in vascular endothelial cells and in RBCs (that will be used in their present study), NO stimulates soluble guanylyl cyclase to produce more cyclic GMP in smooth muscle surrounding blood vessels causing them to relax and increase blood flow through the vasculature. Further functions of NO include its interaction with mitochondrial cytochromes and reduction of respiration, as well as binding of NO to the SH-groups forming S-nitrosylated adducts. Thereby, protein thiols get protected from irreversible oxidation. During oxidative stress, NO functions as an alternative sink for superoxide anion. Fast generation peroxynitrite species (ONOO⁻) overrides production of hydrogen peroxide by superoxide dismutase. The resulting ONOO⁻ is quickly (within seconds) transformed to either NO₃⁻ or interacts with tyrosine residues causing accumulation of nitro-tyrosine adducts.

The effects of temperature alterations on NO production by endothelial NO synthase (eNOS) in RBCs have not been investigated in detail. However, analysis of thermodynamics of reactions involving catalytic NO production by the other isozyme, neuronal NO synthase (nNOS) revealed a temperature-dependent increase in all reaction constants of the NO production process [118]. Heating is discussed as a cause of light-induced improvement of skin capillary perfusion [119]. Furthermore, uptake of Ca²⁺ stimulates NO production catalyzed by iNOS and eNOS [120][121]. In RBCs, NO production is sensitive to mechanical stimulation which activates Ca²⁺ uptake via mechano-sensitive Piezo1 channels [122]. As we have shown, an increase in temperature to 40°C induces Ca²⁺ accumulation in the cells (Figure 7a). Taken together, these findings suggest that NO production in RBCs may be facilitated by heating. A pilot set of experiments was performed to test this hypothesis.

4.4.2 Methods

Whole blood (venous samples, anticoagulated with Li-heparin) is used for the experiments. Plasma is collected to assess the basal concentration of nitrite and nitrate (RNO). Three samples are prepared to assess temperature-dependence of NO production. They are incubated for 40 minutes at three different temperatures (on ice, at 25°C, or at 40°C) while shaking. Thereafter, RBCs are pelleted, and plasma is collected and frozen at -20°C. RNO concentrations is assessed in plasma within the next 1-3 weeks after collection using the chemiluminescence detection technique (for details see [123][124]) Pilot experiments using this method are on the way.

5 Conclusion

A new far-field exposure setup was designed by the HUJI partners in close collaboration with partners from UNICAS and TUD. In addition, the TUD partners designed a generator to produce a unified modulated signal at a frequency of 3.5 GHz. Another system to generate a signal at 26 GHz was in production. The CST modelling of the EMF power distribution in the sample was amended with temperature measurements in the exposure cuvette to finalize the experimental dosimetry. Afterward, the exposure system was shipped to Zurich and installed to be used by the UZH partners by the end of November 2024. Meanwhile, the temperature dependence on the parameters of choice was studied by the UZH and HUJI partners using experimental protocols refined for future RF-EMF experiments.

The data obtained contributed to work within the KPI. According to this KPI, we were required to gather information on the possible responsiveness of at least five blood parameters to RF-EMF. We already determined that Ca^{2+} movements across the RBC membrane might be thermally regulated. Other parameters dependent on intracellular Ca^{2+} include RBC rheology and NO production. Information on the temperature dependence of thiol-disulfide exchange enhanced our understanding of the potential influence (thermal or otherwise) of RF-EMF on the kinetics of this reaction.

As the next step, *ex vivo* experiments were conducted using the new exposure system. The first frequency used for exposure was 3.5 GHz, with or without modulation. The KPI of testing at least five independent RBC parameters for sensitivity to EMF was met. To date, we have tested the following parameters for their sensitivity to temperature changes: hydration state of hemoglobin, interaction of hemoglobin with oxidized glutathione, intraerythrocytic Ca^{2+} levels and transport of Ca^{2+} across the membrane, abundance of reduced protein and non-protein thiols in RBCs, and RBC deformability. Production of NO by erythroid NO synthase, changes in RBC density, and aggregability are scheduled for testing in the future. Subsequently, experiments will be repeated at 26 GHz using the signal generators provided by the TUD partners.

The obtained results and the SOPs developed to generate the data were shared with consortium members and placed in open repositories. The experimental techniques were also used to analyse blood samples obtained from healthy human volunteers in Case Study 3.

References

- [1] Arroyo JI, B Diez, CP Kempes, GB West and PA Marquet. (2022). A general theory for temperature dependence in biology. *Proc Natl Acad Sci U S A* 119:e2119872119.
- [2] Kim KE, SK Park, SY Nam, TJ Han and IY Cho. (2016). Potential therapeutic mechanism of extremely low-frequency high-voltage electric fields in cells. *Technol Health Care* 24:415-27.
- [3] Sam J, M Catapano, S Sahni, F Ma, A Abd-Elseyed and O Visnjevac. (2021). Pulsed Radiofrequency in Interventional Pain Management: Cellular and Molecular Mechanisms of Action - An Update and Review. *Pain Physician* 24:525-532.
- [4] International Commission on Non-Ionizing Radiation P. (2020). Guidelines for Limiting Exposure to Electromagnetic Fields (100 kHz to 300 GHz). *Health Phys* 118:483-524.
- [5] 39 ISCC. (2019). IEEE Standard for Safety Levels with Respect to Human Exposure to Electric, Magnetic, and Electromagnetic Fields, 0 Hz to 300 GHz. IEEE International Committee on Electromagnetic Safety.
- [6] Sheppard AR, ML Swicord and Q Balzano. (2008). Quantitative evaluations of mechanisms of radiofrequency interactions with biological molecules and processes. *Health Phys* 95:365-96.
- [7] The European Commission and its Scientific Committee on Health EaERS. (2022). SCHEER - Public consultation on the Preliminary Opinion on scientific evidence on radiofrequency.
- [8] IEEE. (2019). IEEE Standard for Safety Levels with Respect to Human Exposure to Electric, Magnetic and Electromagnetic Fields, 0 Hz to 300 GHz. IEEE Std C95.1™.
- [9] Scientific Committee on Emerging and Newly Identified Health Risks (SCENIHR). Potential health effects of exposure to electromagnetic fields (EMF). (2015). European Commission, Luxembourg.
- [10] Sheppard AR, ML Swicord and Q Balzano. (2008). Quantitative evaluations of mechanisms of radiofrequency interactions with biological molecules and processes. *Health physics* 95:365-396.
- [11] SRSA. (2019). Recent Research on EMF and Health Risk, Fourteenth report from SSM's Scientific Council on Electromagnetic Fields.
- [12] ICNIRP. (2009). Review of the scientific evidence on dosimetry, biological effects, epidemiological observations, and health consequences concerning exposure to high frequency electromagnetic fields (100 kHz to 300 GHz). ICNIRP.
- [13] Apollonio F, M Liberti, A Paffi, C Merla, P Marracino, A Denzi, C Marino and G d'Inzeo. (2013). Feasibility for microwaves energy to affect biological systems via nonthermal mechanisms: a systematic approach. *IEEE Transactions on Microwave Theory and Techniques* 61:2031-2045.
- [14] Kaatz U. (2015). Dielectric relaxation of water. In: *Dielectric relaxation in biological systems*. Raicu V and Y Feldman, eds. Oxford University Press, Oxford.
- [15] Popov I, PB Ishai, A Khamzin and Y Feldman. (2016). The mechanism of the dielectric relaxation in water. *Phys Chem Chem Phys* 18:13941-53.
- [16] Raicu V and Y Feldman. *Dielectric Relaxation in Biological Systems: Physical Principles, Methods, and Applications*. (2015). Oxford University press, Oxford UK.
- [17] Laage D, T Elsaesser and JT Hynes. (2017). Water Dynamics in the Hydration Shells of Biomolecules. *Chem Rev* 117:10694-10725.
- [18] Marracino P, M Liberti, G d'Inzeo and F Apollonio. (2015). Water response to intense electric fields: A molecular dynamics study. *Bioelectromagnetics* 36:377-85.
- [19] Challis LJ. (2005). Mechanisms for interaction between RF fields and biological tissue. *Bioelectromagnetics Suppl* 7:S98-S106.
- [20] Hochachka PW and GN Somero. *Biochemical Adaptation: Mechanism and Process in Physiological Evolution*. (2002). Oxford University Press.
- [21] Brahm J. (1983). Kinetics of glucose transport in human erythrocytes. *J Physiol* 339:339-54.
- [22] Lacko L, B Wittke and P Geck. (1973). The temperature dependence of the exchange transport of glucose in human erythrocytes. *J Cell Physiol* 82:213-8.
- [23] Hall AC, JC Ellory and RA Klein. (1982). Pressure and temperature effects on human red cell cation transport. *J Membr Biol* 68:47-56.
- [24] Stewart GW, JC Ellory and RA Klein. (1980). Increased human red cell cation passive permeability below 12 degrees C. *Nature* 286:403-4.
- [25] Jennings ML. (1999). Volume-sensitive K(+)/Cl(-) cotransport in rabbit erythrocytes. Analysis of the rate-limiting activation and inactivation events. *J Gen Physiol* 114:743-58.
- [26] Allis JW and BL Sinha-Robinson. (1987). Temperature-specific inhibition of human red cell Na⁺/K⁺ ATPase by 2,450-MHz microwave radiation. *Bioelectromagnetics* 8:203-12.
- [27] Sarkadi B, I Szasz, A Gerloczy and G Gardos. (1977). Transport parameters and stoichiometry of active calcium ion extrusion in intact human red cells. *Biochim Biophys Acta* 464:93-107.

- [28] Wood A and K Karipidis. (2021). Radiofrequency Fields and Calcium Movements Into and Out of Cells. *Radiat Res* 195:101-113.
- [29] Weber RE and KL Campbell. (2011). Temperature dependence of haemoglobin-oxygen affinity in heterothermic vertebrates: mechanisms and biological significance. *Acta Physiol (Oxf)* 202:549-62.
- [30] Mansourian M, SMP Firoozabadi and ZM Hassan. (2021). The effect of 900 MHz electromagnetic fields on biological pathways induced by electrochemotherapy. *Electromagn Biol Med* 40:158-168.
- [31] Mansourian M, SMP Firoozabadi and ZM Hassan. (2022). The investigation of Pulse-Modulated GSM-900 MHz electromagnetic field effects on the electrochemotherapy mechanisms in vivo. *Electromagn Biol Med* 41:71-79.
- [32] Hernansanz-Agustin P, C Choya-Foces, S Carregal-Romero, E Ramos, T Oliva, T Villa-Pina, L Moreno, A Izquierdo-Alvarez, JD Cabrera-Garcia, A Cortes, AV Lechuga-Vieco, P Jadiya, E Navarro, E Parada, A Palomino-Antolin, D Tello, R Acin-Perez, JC Rodriguez-Aguilera, P Navas, A Cogolludo, I Lopez-Montero, A Martinez-Del-Pozo, J Egea, MG Lopez, JW Elrod, J Ruiz-Cabello, A Bogdanova, JA Enriquez and A Martinez-Ruiz. (2020). Na(+) controls hypoxic signalling by the mitochondrial respiratory chain. *Nature* 586:287-291.
- [33] Clarke A and HO Portner. (2010). Temperature, metabolic power and the evolution of endothermy. *Biol Rev Camb Philos Soc* 85:703-27.
- [34] Arcus VL and AJ Mulholland. (2020). Temperature, Dynamics, and Enzyme-Catalyzed Reaction Rates. *Annu Rev Biophys* 49:163-180.
- [35] Paredi P, SA Kharitonov, T Hanazawa and PJ Barnes. (2001). Local vasodilator response to mobile phones. *Laryngoscope* 111:159-62.
- [36] Kaplan JH and LJ Kenney. (1985). Temperature effects on sodium pump phosphoenzyme distribution in human red blood cells. *J Gen Physiol* 85:123-36.
- [37] Powell T, A Noma, T Shioya and RZ Kozlowski. (1993). Turnover rate of the cardiac Na(+)-Ca²⁺ exchanger in guinea-pig ventricular myocytes. *J Physiol* 472:45-53.
- [38] Mackiewicz U and B Lewartowski. (2006). Temperature dependent contribution of Ca²⁺ transporters to relaxation in cardiac myocytes: important role of sarcolemmal Ca²⁺-ATPase. *J Physiol Pharmacol* 57:3-15.
- [39] Dipolo R and R Latorre. (1972). Effect of temperature on membrane potential and ionic fluxes in intact and dialysed barnacle muscle fibres. *J Physiol* 225:255-73.
- [40] Fago A, C Hundahl, S Dewilde, K Gilany, L Moens and RE Weber. (2004). Allosteric regulation and temperature dependence of oxygen binding in human neuroglobin and cytoglobin. *Molecular mechanisms and physiological significance. J Biol Chem* 279:44417-26.
- [41] Lim HJ, YJ Lee, JH Nam, S Chung and S Shin. (2010). Temperature-dependent threshold shear stress of red blood cell aggregation. *J Biomech* 43:546-50.
- [42] Williamson JR, MO Shanahan and RM Hochmuth. (1975). The influence of temperature on red cell deformability. *Blood* 46:611-24.
- [43] Gomez-Pastor R, ET Burchfiel and DJ Thiele. (2018). Regulation of heat shock transcription factors and their roles in physiology and disease. *Nat Rev Mol Cell Biol* 19:4-19.
- [44] Vihervaara A, FM Duarte and JT Lis. (2018). Molecular mechanisms driving transcriptional stress responses. *Nat Rev Genet* 19:385-397.
- [45] Simko M, C Hartwig, M Lantow, M Lupke, MO Mattsson, Q Rahman and J Rollwitz. (2006). Hsp70 expression and free radical release after exposure to non-thermal radio-frequency electromagnetic fields and ultrafine particles in human Mono Mac 6 cells. *Toxicol Lett* 161:73-82.
- [46] Georgiou CD and LH Margaritis. (2021). Oxidative Stress and NADPH Oxidase: Connecting Electromagnetic Fields, Cation Channels and Biological Effects. *Int J Mol Sci* 22.
- [47] Schuermann D and M Mevissen. (2021). Manmade Electromagnetic Fields and Oxidative Stress-Biological Effects and Consequences for Health. *Int J Mol Sci* 22.
- [48] Cotgreave IA. (2005). Biological stress responses to radio frequency electromagnetic radiation: are mobile phones really so (heat) shocking? *Arch Biochem Biophys* 435:227-40.
- [49] Georgiou CD. (2010). Oxidative stress-induced biological damage by low-level EMFs: mechanism of free radical pair electron spinpolarization and biochemical amplification. *Eur J Oncol* 5:63-113.
- [50] Yakymenko I, O Tsybulin, E Sidorik, D Henshel, O Kyrlyenko and S Kyrlyenko. (2016). Oxidative mechanisms of biological activity of low-intensity radiofrequency radiation. *Electromagn Biol Med* 35:186-202.
- [51] Bertagna F, R Lewis, SRP Silva, J McFadden and K Jeevaratnam. (2021). Effects of electromagnetic fields on neuronal ion channels: a systematic review. *Ann N Y Acad Sci*.
- [52] Risks SCoEaNIH and SCENIHR". (2015). Opinion on Potential health effects of exposure to electromagnetic fields (EMF). European Commission Luxembourg.

- [53] Wu H, MR Ghaani, PK Nandi and NJ English. (2022). Investigation of Dipolar Response of the Hydrated Hen-Egg White Lysozyme Complex under Externally Applied Electric Fields: Insights from Non-equilibrium Molecular Dynamics. *J Phys Chem B* 126:858-868.
- [54] Aramouni K, R Assaf, A Shaito, M Fardoun, M Al-Asmakh, A Sahebkar and AH Eid. (2023). Biochemical and cellular basis of oxidative stress: Implications for disease onset. *J Cell Physiol* 238:1951-1963.
- [55] Smith MT and KZ Guyton. (2020). Identifying carcinogens from 10 key characteristics. A new approach based on mechanisms. In: *World Cancer Report: Cancer Research for Cancer Prevention* Wild CP, E Weiderpass and BW Stewart, eds. IARC Press, Lyon.
- [56] Berridge MJ, MD Bootman and HL Roderick. (2003). Calcium signalling: dynamics, homeostasis and remodelling. *Nat Rev Mol Cell Biol* 4:517-29.
- [57] Berridge MJ. (2012). Calcium signalling remodelling and disease. *Biochem Soc Trans* 40:297-309.
- [58] Berridge MJ. (2016). The Inositol Trisphosphate/Calcium Signaling Pathway in Health and Disease. *Physiol Rev* 96:1261-96.
- [59] Elmore S. (2007). Apoptosis: a review of programmed cell death. *Toxicol Pathol* 35:495-516.
- [60] Henschenmacher B, A Bitsch, T de Las Heras Gala, HJ Forman, A Fragoulis, P Ghezzi, R Kellner, W Koch, J Kuhne, D Sachno, G Schmid, K Tsaïoun, J Verbeek and R Wright. (2022). The effect of radiofrequency electromagnetic fields (RF-EMF) on biomarkers of oxidative stress in vivo and in vitro: A protocol for a systematic review. *Environ Int* 158:106932.
- [61] Karipidis K, R Mate, D Urban, R Tinker and A Wood. (2021). 5G mobile networks and health-a state-of-the-science review of the research into low-level RF fields above 6 GHz. *J Expo Sci Environ Epidemiol* 31:585-605.
- [62] Lai H. (2021). Genetic effects of non-ionizing electromagnetic fields. *Electromagn Biol Med* 40:264-273.
- [63] Kocaman A, G Altun, AA Kaplan, OG Deniz, KK Yurt and S Kaplan. (2018). Genotoxic and carcinogenic effects of non-ionizing electromagnetic fields. *Environ Res* 163:71-79.
- [64] Jagetia GC. (2022). Genotoxic effects of electromagnetic field radiations from mobile phones. *Environ Res* 212:113321.
- [65] Vijayalaxmi and TJ Prihoda. (2019). Comprehensive Review of Quality of Publications and Meta-analysis of Genetic Damage in Mammalian Cells Exposed to Non-Ionizing Radiofrequency Fields. *Radiat Res* 191:20-30.
- [66] Vijayalaxmi and TJ Prihoda. (2012). Genetic damage in human cells exposed to non-ionizing radiofrequency fields: a meta-analysis of the data from 88 publications (1990-2011). *Mutat Res* 749:1-16.
- [67] Romeo S, O Zeni, A Sannino, S Lagorio, M Biffoni and MR Scarfi. (2021). Genotoxicity of radiofrequency electromagnetic fields: Protocol for a systematic review of in vitro studies. *Environ Int* 148:106386.
- [68] Pall ML. (2013). Electromagnetic fields act via activation of voltage-gated calcium channels to produce beneficial or adverse effects. *J Cell Mol Med* 17:958-65.
- [69] Pall ML. (2014). Electromagnetic field activation of voltage-gated calcium channels: role in therapeutic effects. *Electromagn Biol Med* 33:251.
- [70] Bertagna F, R Lewis, SRP Silva, J McFadden and K Jeevaratnam. (2021). Effects of electromagnetic fields on neuronal ion channels: a systematic review. *Ann N Y Acad Sci* 1499:82-103.
- [71] Romeo S, O Zeni, MR Scarfi, L Poeta, MB Lioi and A Sannino. (2022). Radiofrequency Electromagnetic Field Exposure and Apoptosis: A Scoping Review of In Vitro Studies on Mammalian Cells. *Int J Mol Sci* 23.
- [72] Latypova L, A Puzenko, E Levy and Y Feldman. (2020). Dielectric spectra broadening as a signature for dipole-matrix interactions. V. Water in protein solutions. *J Chem Phys* 153:045102.
- [73] Mousavy SJ, GH Riazi, M Kamarei, H Aliakbarian, N Sattarahmady, A Sharifizadeh, S Safarian, F Ahmad and AA Moosavi-Movahedi. (2009). Effects of mobile phone radiofrequency on the structure and function of the normal human hemoglobin. *Int J Biol Macromol* 44:278-85.
- [74] Feng C. (2012). Mechanism of Nitric Oxide Synthase Regulation: Electron Transfer and Interdomain Interactions. *Coord Chem Rev* 256:393-411.
- [75] Pauling L. (1977). Magnetic properties and structure of oxyhemoglobin. *Proc Natl Acad Sci U S A* 74:2612-3.
- [76] Beyer C, P Christen, I Jelesarov and J Frohlich. (2014). Real-time assessment of possible electromagnetic-field-induced changes in protein conformation and thermal stability. *Bioelectromagnetics* 35:470-8.
- [77] Chowdhury A, Y Singh, U Das, D Waghmare, R Dasgupta and SK Majumder. (2021). Effects of mobile phone emissions on human red blood cells. *J Biophotonics*:e202100047.
- [78] Bogdanova A, A Makhro, J Wang, P Lipp and L Kaestner. (2013). Calcium in red blood cells-a perilous balance. *Int J Mol Sci* 14:9848-72.

- [79] Kaestner L, A Bogdanova and S Egee. (2020). Calcium Channels and Calcium-Regulated Channels in Human Red Blood Cells. *Adv Exp Med Biol* 1131:625-648.
- [80] Kaestner L, W Tabellion, E Weiss, I Bernhardt and P Lipp. (2006). Calcium imaging of individual erythrocytes: problems and approaches. *Cell Calcium* 39:13-9.
- [81] Rotordam MG, E Fermo, N Becker, W Barcellini, A Bruggemann, N Fertig, S Egee, M Rapedius, P Bianchi and L Kaestner. (2019). A novel gain-of-function mutation of Piezo1 is functionally affirmed in red blood cells by high-throughput patch clamp. *Haematologica* 104:e179-e183.
- [82] Fermo E, A Bogdanova, P Petkova-Kirova, A Zaninoni, AP Marcello, A Makhro, P Hanggi, L Hertz, J Danielczok, C Vercellati, N Mirra, A Zanella, A Cortelezzi, W Barcellini, L Kaestner and P Bianchi. (2017). 'Gardos Channelopathy': a variant of hereditary Stomatocytosis with complex molecular regulation. *Sci Rep* 7:1744.
- [83] Hanggi P, A Makhro, M Gassmann, M Schmugge, JS Goede, O Speer and A Bogdanova. (2014). Red blood cells of sickle cell disease patients exhibit abnormally high abundance of N-methyl D-aspartate receptors mediating excessive calcium uptake. *Br J Haematol* 167:252-64.
- [84] Makhro A, I Hegemann, E Seiler, G Simionato, V Claveria, N Bogdanov, C Sasselli, P Torgeson, L Kaestner, MG Manz, JS Goede, M Gassmann and A Bogdanova. (2020). A pilot clinical phase II trial MemSID: Acute and durable changes of red blood cells of sickle cell disease patients on memantine treatment. *eJHaem* 1:23-34.
- [85] Makhro A, L Kaestner and A Bogdanova. (2017). NMDA Receptor Activity in Circulating Red Blood Cells: Methods of Detection. *Methods Mol Biol* 1677:265-282.
- [86] Dey K, AM van Cromvoirt, I Hegemann, JS Goede and A Bogdanova. (2024). Role of Piezo1 in Terminal Density Reversal of Red Blood Cells. *Cells* 13.
- [87] Huisjes R, A Bogdanova, WW van Solinge, RM Schiffelers, L Kaestner and R van Wijk. (2018). Squeezing for Life - Properties of Red Blood Cell Deformability. *Front Physiol* 9:656.
- [88] Larkin SK, C Hernandez, EJ van Beers, R van Wijk and FA Kuypers. (2024). The RoxyScan is a novel measurement of red blood cell deformability under oxidative and shear stress. *Sci Rep* 14:6344.
- [89] Zaninoni A, E Fermo, C Vercellati, D Consonni, AP Marcello, A Zanella, A Cortelezzi, W Barcellini and P Bianchi. (2018). Use of Laser Assisted Optical Rotational Cell Analyzer (LoRRca MaxSis) in the Diagnosis of RBC Membrane Disorders, Enzyme Defects, and Congenital Dyserythropoietic Anemias: A Monocentric Study on 202 Patients. *Front Physiol* 9:451.
- [90] Barshtein G, TL Rasmusen, O Zelig, D Arbell and S Yedgar. (2020). Inter-donor variability in deformability of red blood cells in blood units. *Transfus Med* 30:492-496.
- [91] Havas M. (2013). Radiation from wireless technology affects the blood, the heart, and the autonomic nervous system. *Rev Environ Health* 28:75-84.
- [92] Tang M-C, T Wang, T Deng and RW Ziolkowski. (2016). Compact Planar Ultrawideband Antennas With Continuously Tunable, Independent Band-Notched Filters. *IEEE Transactions on antennas and propagation* 64:3292 - 3301.
- [93] Kukulage DSK, NNJ Matarage Don and YH Ahn. (2022). Emerging chemistry and biology in protein glutathionylation. *Curr Opin Chem Biol* 71:102221.
- [94] Oppong D, W Schiff, MC Shivamadu and YH Ahn. (2023). Chemistry and biology of enzymes in protein glutathionylation. *Curr Opin Chem Biol* 75:102326.
- [95] Alvarez B, AC Comini, G Salinas and M Trujillo. *Redox Chemistry and Biology of Thiols*. (2022). Academic Press.
- [96] Giustarini D, I Dalle-Donne, A Milzani, D Braconi, A Santucci and R Rossi. (2019). Membrane Skeletal Protein S-Glutathionylation in Human Red Blood Cells as Index of Oxidative Stress. *Chem Res Toxicol* 32:1096-1102.
- [97] Mawatari S and K Murakami. (2004). Different types of glutathionylation of hemoglobin can exist in intact erythrocytes. *Arch Biochem Biophys* 421:108-14.
- [98] Bogdanova A, IY Petrushanko, P Hernansanz-Agustin and A Martinez-Ruiz. (2016). "Oxygen Sensing" by Na,K-ATPase: These Miraculous Thiols. *Front Physiol* 7:314.
- [99] D'Annibale V, D Fracassi, P Marracino, G D'Inzeo and M D'Abramo. (2022). Effects of Environmental and Electric Perturbations on the pKa of Thioredoxin Cysteine 35: A Computational Study. *Molecules* 27.
- [100] Colombo G, I Dalle-Donne, D Giustarini, N Gagliano, N Portinaro, R Colombo, R Rossi and A Milzani. (2010). Cellular redox potential and hemoglobin S-glutathionylation in human and rat erythrocytes: A comparative study. *Blood Cells Mol Dis* 44:133-9.
- [101] Metere A, E Iorio, G Scorza, S Camerini, M Casella, M Crescenzi, M Minetti and D Pietraforte. (2014). Carbon monoxide signaling in human red blood cells: evidence for pentose phosphate pathway activation and protein deglutathionylation. *Antioxid Redox Signal* 20:403-16.

- [102] Craescu CT, C Poyart, C Schaeffer, MC Garel, J Kister and Y Beuzard. (1986). Covalent binding of glutathione to hemoglobin. II. Functional consequences and structural changes reflected in NMR spectra. *J Biol Chem* 261:14710-6.
- [103] Garel MC, C Domenget, J Caburi-Martin, C Prehu, F Galacteros and Y Beuzard. (1986). Covalent binding of glutathione to hemoglobin. I. Inhibition of hemoglobin S polymerization. *J Biol Chem* 261:14704-9.
- [104] Sampathkumar R, M Balasubramanyam, S Sudarslal, M Rema, V Mohan and P Balaram. (2005). Increased glutathionylated hemoglobin (HbSSG) in type 2 diabetes subjects with microangiopathy. *Clin Biochem* 38:892-9.
- [105] Khazim K, D Giustarini, R Rossi, D Verkaik, JE Cornell, SE Cunningham, M Mohammad, K Trochta, C Lorenzo, F Folli, S Bansal and P Fantì. (2013). Glutathione redox potential is low and glutathionylated and cysteinylated hemoglobin levels are elevated in maintenance hemodialysis patients. *Transl Res* 162:16-25.
- [106] Muscat JE, W Kleinman, S Colosimo, A Muir, P Lazarus, J Park and JP Richie, Jr. (2004). Enhanced protein glutathiolation and oxidative stress in cigarette smokers. *Free Radic Biol Med* 36:464-70.
- [107] Cossins AR, PJ Schwarzbau and W Wieser. (1995). Effects of temperature on cellular ion regulation and membrane transport systems In: *Biochemistry and molecular biology of fishes*. Hochachka PW and TP Mommsen, eds. Elsevier Science, pp 100-126.
- [108] Vodyanoy V. (2015). Thermodynamic evaluation of vesicles shed by erythrocytes at elevated temperatures. *Colloids Surf B Biointerfaces* 133:231-8.
- [109] Windberger U, R Auer, R Plasenzotti, S Eloff and JA Skidmore. (2018). Temperature dependency of whole blood viscosity and red cell properties in desert ungulates: Studies on scimitar-horned oryx and dromedary camel. *Clin Hemorheol Microcirc* 69:533-543.
- [110] Zipp A, TL James, ID Kuntz and SB Shohet. (1976). Water proton magnetic resonance studies of normal and sickle erythrocytes. Temperature and volume dependence. *Biochim Biophys Acta* 428:291-303.
- [111] Rendell MS, ST Kelly, O Bamisedun, T Luu, DA Finney and S Knox. (1993). The effect of increasing temperature on skin blood flow and red cell deformability. *Clin Physiol* 13:235-45.
- [112] Nash GB and HJ Meiselman. (1985). Alteration of red cell membrane viscoelasticity by heat treatment: effect on cell deformability and suspension viscosity. *Biorheology* 22:73-84.
- [113] Matrai AA, G Varga, B Tanczos, B Barath, A Varga, L Horvath, Z Bereczky, A Deak and N Nemeth. (2021). In vitro effects of temperature on red blood cell deformability and membrane stability in human and various vertebrate species. *Clin Hemorheol Microcirc* 78:291-300.
- [114] Liu ZL, H Li, Y Qiang, P Buffet, M Dao and GE Karniadakis. (2021). Computational modeling of biomechanics and biorheology of heated red blood cells. *Biophys J* 120:4663-4671.
- [115] Van Cromvoirt AM, S Fenk, A Sadafi, EV Melnikova, DA Lagutkin, K Dey, IY Petrushanko, I Hegemann, JS Goede and A Bogdanova. (2021). Donor Age and Red Cell Age Contribute to the Variance in Lorrca Indices in Healthy Donors for Next Generation Ektacytometry: A Pilot Study. *Front Physiol* 12:639722.
- [116] Barshtein G, A Gural, O Zelig, D Arbell and S Yedgar. (2020). Unit-to-unit variability in the deformability of red blood cells. *Transfus Apher Sci* 59:102876.
- [117] Barshtein G, L Livshits, A Gural, D Arbell, R Barkan, I Pajic-Lijakovic and S Yedgar. (2024). Hemoglobin Binding to the Red Blood Cell (RBC) Membrane Is Associated with Decreased Cell Deformability. *Int J Mol Sci* 25.
- [118] Haque MM, J Tejero, M Bayachou, ZQ Wang, M Fadlalla and DJ Stuehr. (2013). Thermodynamic characterization of five key kinetic parameters that define neuronal nitric oxide synthase catalysis. *FEBS J* 280:4439-53.
- [119] Barolet AC, IV Litvinov and D Barolet. (2021). Light-induced nitric oxide release in the skin beyond UVA and blue light: Red & near-infrared wavelengths. *Nitric Oxide* 117:16-25.
- [120] Patruno A, S Tabrez, M Pesce, S Shakil, MA Kamal and M Reale. (2015). Effects of extremely low frequency electromagnetic field (ELF-EMF) on catalase, cytochrome P450 and nitric oxide synthase in erythro-leukemic cells. *Life Sci* 121:117-23.
- [121] Pilla AA. (2012). Electromagnetic fields instantaneously modulate nitric oxide signaling in challenged biological systems. *Biochem Biophys Res Commun* 426:330-3.
- [122] Ulker P, L Sati, C Celik-Ozenci, HJ Meiselman and OK Baskurt. (2009). Mechanical stimulation of nitric oxide synthesizing mechanisms in erythrocytes. *Biorheology* 46:121-32.
- [123] Kleinbongard P, R Schulz, T Rassaf, T Lauer, A Dejam, T Jax, I Kumara, P Gharini, S Kabanova, B Ozuyaman, HG Schnurch, A Godecke, AA Weber, M Robenek, H Robenek, W Bloch, P Rosen and M Kelm. (2006). Red blood cells express a functional endothelial nitric oxide synthase. *Blood* 107:2943-51.
- [124] Mihov D, J Vogel, M Gassmann and A Bogdanova. (2009). Erythropoietin activates nitric oxide synthase in murine erythrocytes. *Am J Physiol Cell Physiol* 297:C378-88.

